Towards a less biased dissolution of chitosan

Joel J Thevarajah, Jerikho C Bulanadi, Manfred Wagner, Marianne Gaborieau, Patrice Castignolles

Highlights

- Clear solutions of chitosan do not ensure complete solubility
- Aggregation of chitosan is observed in size-exclusion chromatography conditions
- HCl and DCl cause deacetylation of chitosan during dissolution in water
- The extent of chitosan dissolution is more limited in aqueous acetic acid than in aqueous HCl
- The dissolution of chitosan in aqueous HCl is relatively quick; however, it may not be complete

Graphical abstract

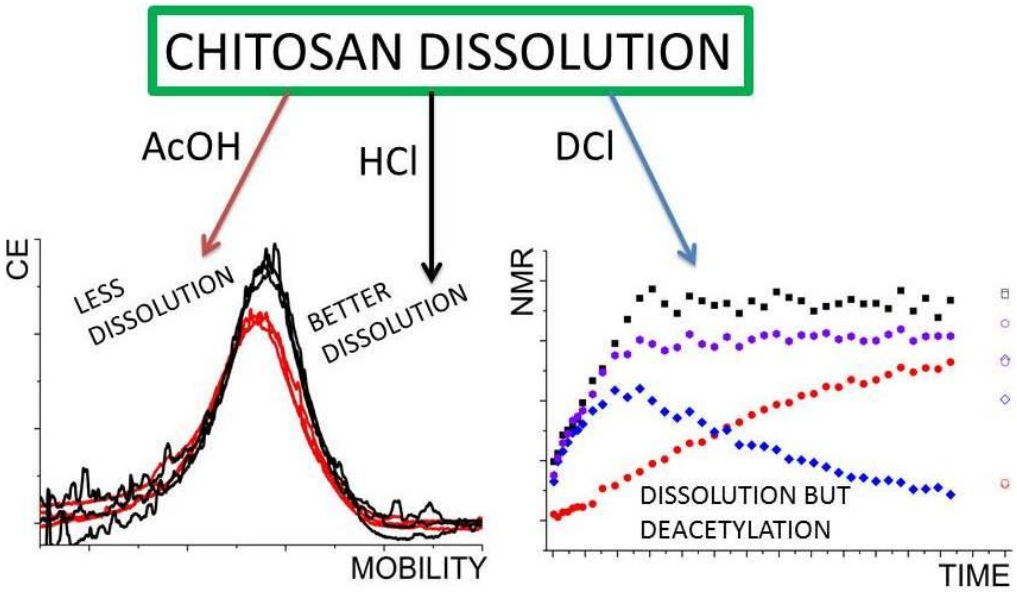

Towards a less biased dissolution of chitosan

Joel J. Thevarajah [a,b,c], Jerikho C. Bulanadi [a], Manfred Wagner [c], Marianne Gaborieau [a,b]*, Patrice Castignolles [a]

[a] Western Sydney University, School of Science and Health, Australian Centre for Research on Separation Sciences (ACROSS), Parramatta, 2150, Australia

[b] Western Sydney University, Molecular Medicine Research Group (MMRG), School of Science and Health, Parramatta, 2150, Australia

[c] Max Planck Institute for Polymer Research, 55128 Mainz, Ackermannweg 10, Germany

*Corresponding author : Marianne Gaborieau, m.gaborieau@westernsydney.edu.au

Abstract

The dissolution of polysaccharides is notoriously challenging, especially when one needs a "true" solution. Factors influencing chitosan's solubility include composition, also known as degree of acetylation (*DA*). The dissolution of chitosan was investigated by visual observation, size-exclusion chromatography (SEC), pressure mobilization (PM), free-solution capillary electrophoresis (CE) and real-time solution-state NMR spectroscopy. Aqueous HCl dissolves around 15 % more chitosan than the commonly used aqueous acetic acid (AcOH), however aggregates were detected in SEC suggesting incomplete dissolution. Significant deacetylation of chitosan over the period needed for dissolution at high temperature occurred in DCl (NMR) by about 20 % of the initial DA value. Accurate *DA* determination by NMR spectroscopy may thus be possible only in the solid state (with a precision within 1 % on the *DA* % scale above a DA of 10 %). Overall a compromise between maximum solubilization and minimum degradation is required in attempting to obtain a "true" solution of chitosan. The completeness of the dissolution may be more influenced by the average *DA* than by molar mass.

Keywords

Chitosan, dissolution, solid-state NMR spectroscopy, solution-state NMR spectroscopy. capillary electrophoresis, size-exclusion chromatography (SEC)

1. Introduction

Chitosan is a polysaccharide derived from the *N*-deacetylation of chitin. Chitin is the second most abundant polysaccharide in the world (by volume after cellulose) and is synthesized by many organisms.[1] Its natural occurrence includes the exoskeletons of arthropods such as shrimps, crabs and the cell walls of yeasts.[2] It is a major waste product of the seafood industry. Its most promising derivative, chitosan, was shown to be biocompatible, biodegradable and antimicrobial, which make it an appropriate material for biomedical applications such as stem cell growth substrate.[3, 4] Chitosan's structure contains varying proportions of D-glucosamine and *N*-acetyl-D-glucosamine units. The degree of acetylation (*DA*) of chitosan refers to the proportion of the *N*-acetyl-D-glucosamine monomer units. It is often characterized only by its average *DA* which does not take into account the complex arrangement of monomer units along the polymer chain.[5] The *DA* and the distribution of the acetyl groups along chitosan chains affect the dissolution or hydrolysis of chitosan.[6, 7]

A significant factor that hinders a meaningful characterization of chitosan is the difficulty to fully dissolve it without degrading it. To allow for the proper separation and characterization of a polysaccharide (by chromatography, light scattering, etc.), true solutions are required as in the case of starch.[8] A true (dilute) solution is defined in this work as a solution where all macromolecules (chitosan chains) are surrounded by solvent molecules [9]. True solutions are also necessary to allow the homogenous chemical modification of chitosan.[10] The dissolution of polysaccharides is generally complex, and various techniques have been used to assess it in different ways. A dissolved sample will visually appear as a clear and transparent liquid; however, obtaining a clear and transparent liquid does not always mean that the sample

is completely dissolved. In the case of starch, quantitative ^{1}H NMR spectroscopy of a transparent liquid proved it to contain undissolved starch (up to 15 % of the initial starch) for some starches possibly due to the presence of aggregates which were invisible to the naked eye.[8] Unlike chitin, which is largely insoluble in aqueous and organic solvents, chitosan is partially soluble owing to the amine group of its D-glucosamine monomer. However, the actual extent of dissolution of chitosan is often overlooked and is dependent on structural characteristics including the distributions of the degrees of acetylation and environmental conditions such as pH, ionic strength, temperature, time and the dielectric constant of the solvent.[3, 11] UV spectrophotometry at 600 nm has been used to analyse the dissolution by analysis of the turbidity, however this overlooks the presence of aggregates or non-dissolved parts of the chitosan small enough to produce minimal scattering of visible light.[12] A range of methods has been used to monitor the dissolution of macromolecules [9], but a number of these methods do not discriminate between true solution and dispersion (aggregation) such as viscometry,[13] FT-IR spectroscopy [14], or pyrolysis gas chromatography [15, 16].

Light scattering (static and dynamic) was used to analyse the dissolution of chitosan, unfortunately, there were several limitations. Chitosan dissolution is often complicated by the presence of (concentration dependent) aggregation. Common methods to remove aggregates are ultracentrifugation and filtration. However, in the case of chitosan, these methods were shown to remove high molar mass chains and caused the light scattering results to be strongly influenced by the filtering procedure undertaken.[17] Size-exclusion chromatography (SEC) coupled to multi-angle light scattering (MALS) identified aggregation in chitosan samples and heterogeneity of the solution [18]. It was further identified that the aggregates are stable in solutions and thus light scattering cannot accurately characterize chitosan.[17, 18] The extent of the aggregation did not correlate with the average *DA* in this work.

SEC is a commonly used method in the characterization of polysaccharides.[19] It has been used in an attempt to obtain molar mass distributions of chitosan.[2] Unfortunately, as identified previously, chitosan's poor solubility and aggregation causes difficulty in choosing an appropriate solvent. Solvents such as 0.1 M acetic acid/0.2 M sodium chloride were shown to cause an overestimation of molar mass due to the promotion of aggregation. It was also noted that light scattering was sensitive to the aggregation of highly acetylated chitosan samples.[20]

Beyond light scattering, Taylor dispersion analysis (TDA) can be used to determine the diffusion coefficient of macromolecules, but has never been applied to chitosan. The diffusion coefficient is related to the size of the macromolecules and thus TDA can provide information regarding the presence of aggregates or dissolved molecules. The detection of narrow and broad peaks allow a clear distinction between the dissolved sample and aggregate formation.[21] Free-solution capillary electrophoresis (CE) or capillary zone electrophoresis has been applied in a limited but successful fashion to the characterization of polysaccharides, including the separation of chitosan samples by their *DA*.[5, 22] CE proved to separate the samples by their *DA* with no sample preparation required, not even sample filtration. The area of the peaks on the CE electropherograms could thus be used to analyse the dissolution of chitosan, with no bias due to sample preparation. It is important to note that aggregates, as long as their diffusion coefficient is much lower than that of the macromolecules of interest, lead to very sharp peaks in CE. These sharp peaks are easily distinguished from the polymer peak as in the case of gellan gum [23].

In this paper the dissolution of chitosan samples is investigated with various techniques: capillary electrophoresis and pressure mobilization, multiple-detection SEC, as well as solution-state and solid-state NMR spectroscopy. Aggregation, extent of dissolution and possible chemical degradation are assessed.

2. Experimental

2.1. Materials

Chitosan powders were purchased from Aldrich, Castle Hill, Australia and from AK Biotech, Jinan, China (Table 1). Samples were prepared at 1 $g \cdot L^{-1}$. Orthophosphoric acid (85 %) was purchased from BDH AnalR, Merck Pty Ltd. Acetic acid (AcOH, glacial, 99 %) and hydrochloric acid (32 %) were purchased from Unilab. Sodium hydroxide pellets, sodium chloride, trifluoroacetic acid (TFA, 99 %), Hexaamminecobalt(III) chloride (≥99.5 %), dimethyl sulfoxide (DMSO, 99 %) and adamantane (99 %) were purchased from Sigma-Aldrich. Deuterium chloride (35 %) was purchased from Cambridge Isotope Laboratories. All water used in this study was of Milli-Q quality. The SEC eluent was prepared from TFA at 0.3% (w/v) with 0.1 M NaCl. The eluent was filtered with 0.22 µm Nylon 6,6 filter. Nine pullulan standards (with weight-average molar masses between 342 and 805,000 $g \cdot mol^{-1}$ and dispersity values between 1.00 and 1.27) were purchased from Polymer Standard Service, Mainz, Germany. Sodium borate buffer (75 mM) was prepared from 0.5 M boric acid in Milli-Q water, titrated to pH 9.20 with 10 M sodium hydroxide, and diluted with Milli-Q water. Sodium phosphate buffer (100 mM) was prepared from 0.5 M sodium dihydrogen phosphate, titrated with phosphoric acid, and diluted with Milli-Q water. Sodium borate and phosphate buffers were sonicated for 5 min and filtered with a Whatman (0.2 µm) or Millex GP PES syringe filter (0.22 µm) before use.

2.2. Capillary electrophoresis and pressure mobilization

Free-solution capillary electrophoresis (CE) and pressure mobilization (PM) experiments were carried out using an Agilent 7100 CE (Agilent Technologies, Waldbronn, Germany) instrument equipped with a diode array detector and external circulating bath with MX temperature controller (Polyscience, USA). Polyimide-coated fused silica high sensitivity capillaries (50 µm internal diameter) were purchased from Agilent. The capillary (104 cm

total length, 95.5 cm effective length) was initially pretreated by flushing with 1 M NaOH for 10 min, then with 0.1 M NaOH, Milli-Q water and sodium phosphate buffer for 5 min each at the start of the series of experiments. An oligo(sodium acrylate) was separated [24] in sodium borate (75 mM, pH 9.3) to validate the capillary and the instrument before each session. The electrolyte for chitosan analysis was sodium phosphate (100 mM, pH 2 or 3). Before each experiment the capillary was rinsed with HCl (50 mM) and sodium phosphate (100 mM, pH 2 or 3) for 5 min respectively. Hydrodynamic injections for PM were carried out with 75 mbar for 10 s and for capillary electrophoresis with 40 mbar for 20 s (both corresponding to injection volumes of 0.14 % of the total capillary volume, see Eq. S1 in supporting information). CE was undertaken by applying 30 kV at 25 or 55 °C. PM was undertaken at a pressure of 75 mbar (without electric field). For PM the sample was mixed with the background electrolyte with the electric field. This involved ramping voltage up to 30 kV and then down to -30 kV and back up to 0 kV over the first 4 min of separation (Fig S-3). The mixing of the chitosan with the carrier liquid is due to the electroneutrality of the solution needing to be maintained at all times, even during the ramping process. This is possible due to the reservoirs of buffer which represent an infinite source of the liquid carrier's ions compared to the capillary volume. As the anions and cations of the buffer migrate with the electric field, the counter-ions migrate as well to maintain electroneutrality which results in mixing. When the electric field is off, the sample is allowed to migrate through the capillary within the carrier liquid. Pressure-assisted capillary electrophoresis (PACE) was undertaken with both an electric field (30 kV) and pressure (50 mbar) at 55 °C. For kinetic measurements undertaken using PACE, the CE carousel was kept at 60 °C using an external circulating bath. Detection was set at 195 nm. All CE and PM data were treated with the software Origin 9 and the x and y axes were normalized based on previous studies [25, 26], converting the y axis into a time-corrected y axis $h(t)$, or a weight distribution of electrophoretic mobilities $W(\mu)$ (see supporting information).

2.3. Multiple-detection size-exclusion chromatography

The analysis of chitosan was undertaken with a Malvern Viscotek triple-detector size-exclusion chromatography instrument triple detector array consisting of an online degasser, pump, automatic sample injector, one precolumn and three NOVEMA columns (one low molar mass column: 30 Å and two medium molar mass columns: 1 000 Å, both with particle sizes of 10 µm) from Polymer Standards Service, Mainz, Germany. The triple detector array included in series RALS (right-angle light scattering, 670 nm), refractometer (660 nm) and viscometer thermostated at 50 °C, controlled by the software OmniSEC. The flow rate was 0.85 $mL \cdot min^{-1}$. Ethylene glycol was used as a flow rate marker and the injection volume was set at 100 µL. The eluent was regularly injected to check for the absence of system peaks on all the detectors' signals and the absence of bleeding from the columns.

2.4. Solid-state NMR spectroscopy

Solid-state ^{1}H and ^{13}C NMR spectra were recorded on a Bruker Avance DPX200 spectrometer operating at Larmor frequencies of 200 MHz and 50 MHz, respectively. A commercial double resonance probe supporting zirconia MAS rotors with a 4 mm outer diameter and a 3 mm inner diameter was used, and samples were spun at 10 kHz at the magic angle. ^{1}H experiments were recorded using a 90 $^{\circ}$ pulse, a 3 s repetition delay with at least 64 scans accumulated. ^{13}C CP-MAS NMR experiments were adapted from quantitative measurements found in the literature [27, 28]. They were recorded with a 1 ms contact time and a 4 s repetition delay, and 21,586 to 104,924 scans. For ^{1}H experiments the 90 $^{\circ}$ pulse was optimized using adamantane and power levels for the ^{13}C CP-MAS experiments were optimized using a mixture of three ^{13}C singly labeled alanines. The ^{1}H and ^{13}C chemical shifts scales were externally referenced using adamantane by setting the CH resonance to 1.64 and 38.48 ppm, respectively [29]. The degree of acetylation was measured through Eq. 1 [27]:

$$DA_n^{SSNMR}(\%) = \frac{I_{CH_3}}{(I_1+I_2+I_3+I_4+I_5+I_6)/6} \quad (1)$$

Where I_{CH3} is the integral of the methyl group of the acetyl group and I_1-I_6 are the integrals of the signals assigned to the chitosan backbone.

To measure the deacetylation by solid-state NMR spectroscopy 250 mg chitosan (MedMW1) was dissolved at 1 gL^{-1} in 50 mM HCl in Milli-Q water or in 50 mM DCl in D_2O. Each sample was then kept in an oven at 60 °C for 55 h. After removing the sample from the oven the dispersion was neutralized with excess 1M NaOH. The dispersion was then filtered and rinsed with 500 mL of Milli-Q water, freeze-dried and measured by solid-state NMR spectroscopy.

2.5. Solution-state NMR spectroscopy

The kinetic measurements were recorded on a Bruker 500 MHz Avance III system operating at a Larmor frequency of 500 MHz, equipped with a 5 mm z-gradient BBFO 1H/X probe with z-gradient using TopSpin 3.2 (Bruker). The ^1H NMR spectra were measured in deuterium oxide at 333 K. The accuracy of the temperature was controlled with a methanol sample. The sample was prepared at 1 $g{\cdot}L^{-1}$ in approximately 0.8 M DCl in D_2O. A standard kinetic ^1H NMR experiment was started immediately after the chitosan was mixed with solvent, and recorded with 32 transients per spectrum with a 10.6 µs 90° pulse, a spectral width of 11,000 Hz and a repetition delay of 8.6 s (3.6 s acquisition time and 5 s relaxation delay). A total of 800 successive spectra were recorded over 61 h. The relaxation rate (T_1) of the protons was measured before and after the kinetic run with the inversion recovery method and the T_1 values for the acetyl peak and the peak associated to the backbone were determined to be 1.2 s and 943 ms, respectively. Therefore the kinetic experiment conducted was quantitative. Repeat monitoring experiments were conducted on a Bruker DRX300 spectrometer operating at a Larmor frequency of 300.13 MHz equipped with a 5-mm dual $^1H/^{13}C$ probe at 333 K. The temperature was calibrated with 80 % glycol in DMSO. The measurements were undertaken

with 64 transients per spectrum with a 1.7 µs 30° pulse and a repetition delay of 18.3 s (4.3 s acquisition time and 14 s relaxation delay).

The solution-state NMR measurements for quantifying *DA* conditions were as previously [5].

3. Results and discussion

3.1. Visual observation of dissolution

Pillai [11] suggested that the dissolution of chitosan does not occur in inorganic solvents and therefore the first qualitative measurement of the dissolution of chitosan was through visual observation in aqueous solvents (also more suitable for biomedical applications). Chitosan can be soluble only at a pH below 6.[11] Aqueous solvents (Table S1) were used at different acid concentrations, limiting them to low concentrations to prevent chitosan degradation. No dissolution took place at 5 mM or 10 mM hydrochloric, acetic, trifluoroacetic, phosphoric, and boric acid. 50 mM concentration of hydrochloric, trifluoroacetic or acetic acid produced clear transparent suspensions after 15 min at room temperature. Trifluoracetic acid has been suggested to be more effective at dissolving chitosan but also samples with a higher *DA*.[30] Phosphoric and boric acid even at higher concentrations were unable to produce a visually clear sample. The acids that were unable to produce a clear solution at room temperature were tested at higher temperatures (Table S2 and Table 1). It was observed that only phosphoric acid was able to produce a clear solution if it was left at 60 °C for 1 h. Using the conditions previously established other chitosan samples with a range of different average *DA*s were also evaluated visually for dissolution in HCl 50 mM, TFA 0.3 % and SEC eluent at 60 °C for 2 h. Samples that were not visually dissolved were left overnight on a shaker at room temperature (Table 1). It was concluded from the visual observations that different samples varied in the time needed to produce a clear suspension. This confirmed that the dissolution process was complex and further analysis was required.

3.2. Size-exclusion chromatography and aggregation

SEC is the gold standard for the characterization of polymers especially for the determination of molar mass distributions. This, as well as the degradation and oligomers of chitosan, was characterized using SEC equipped with PSS NOVEMA columns [31-33]. Aqueous HCl was not chosen to prevent the corrosion of the SEC instrument. A TFA-based eluent was indicated as an appropriate running buffer for the PSS NOVEMA columns for chitosan by PSS in an application note [34]. In this study SEC was used to analyze chitosan samples with different *DA*s. Pullulans were used as standards to generate a conventional calibration curve (Figure S-1). Pullulan-equivalent molar masses of the chitosan samples (Table S3) were repeatable, but not reproducible, as commonly observed in SEC.[35] The reproducibility was investigated only by varying the injection concentration, but this already led to significant variations as observed for other polysaccharides.[36] Importantly, the determined apparent molar masses were 7 orders of magnitude larger than that of the largest pullulan standard. The values obtained are physically impossible, well beyond the experimental error associated to pullulan-equivalent (or any apparent) molar masses [37]. This is likely explained by aggregation in these conditions as observed also with other SEC conditions.[18] Analysis of the refractive index and right angle light scattering detector traces (Fig. 1) revealed that all chitosan samples were bimodal. The different samples exhibited 2 different populations and bimodal peaks: a peak at a lower elution time and a peak at a higher elution time. The peak at a low elution time infers a large molar mass and is assigned to the aggregates and the peak at a higher elution time is inferred to be the dissolved chitosan. The large molar mass values obtained and the intensity of the LS signal which is sensitive to large molar masses [38] were in good agreement of the existence of aggregation.

Samples that exhibited a separation of aggregates and dissolved polymer (analysis of elution profile) were then diluted (up to 1/100) to assist in breaking apart the aggregates. However,

the aggregation remained in the diluted sample suggesting a high stability (Fig. 1B) as suggested in the case of starch.[39]

3.3. Evaluation of dissolution by pressure mobilization

Chitosan MedMW1 dissolved in aqueous HCl and AcOH was chosen to be analyzed by pressure mobilization (PM) based on initial visual observations. The sample was heated for 2 h at 60 °C to ensure a clear liquid was obtained. PM is used for the first time to analyze the dissolution of chitosan. It was initially performed with phosphate buffer at pH 3 at 25 ºC as the carrier liquid without mixing of the chitosan suspension with the phosphate buffer. A large peak with considerable tailing was observed for chitosan dissolved in aqueous HCl and a small peak with tailing for the chitosan dissolved in aqueous AcOH (Fig. S2). The large UV absorbance of the sample dissolved in HCl is uncharacteristic of chitosan; however, the presence of tailing suggests adsorption onto the capillary surface [40]. Repeatable results were obtained with the sample dissolved in HCl; however, samples dissolved in AcOH exhibited adsorption and poor repeatability. Therefore conditions were adapted and PM experiments were carried out with a slightly different carrier liquid of pH 2 phosphate buffer (100 mM) with mixing (Fig. 2) at 55 ºC. The mixing involved the adjustment of the electric field between 30 kV and -30 kV (Fig. S3) immediately after the injection and the addition of pressure (which was reduced from 72 mbar to 63 mbar). Chitosan dissolved in HCl produced 2 signals slightly separated from each other and the blank (no chitosan) produced a large signal from HCl 50 mM (Fig. 2A). The large signal was assigned to the Cl^- from HCl [41]. To analyze the chitosan signal the intensity of the Cl^- signal was normalized based on the viscosity difference between the solutions (Eq. S2). The peak of Cl^- has similar migration to blanks with injection of the carrier liquid spiked with DMSO. The injection of 50 mM HCl was then superimposed and subtracted from the chitosan dissolved in 50 mM HCl (Fig. 2B). The remaining peak is identified as chitosan. The unexpected separation of chitosan and Cl^-

may be due to the occurrence of ion exclusion of the Cl^- and the adsorption of the chitosan. Tailing toward high elution times, indicative of slight adsorption [40] could still be seen; however, this was less pronounced than for chitosan dissolved in 50 mM AcOH.
Chitosan dissolved in aqueous AcOH exhibited a sharp peak (also present in the blank) coeluting with a broad peak. The sharp peak is thus assigned to acetate. The area of the chitosan dissolved in AcOH was calculated by integrating the chitosan with the acetate peak superimposed and subtracting the peak area of the acetate peak (Fig. S4). The peak area of chitosan dissolved in aqueous HCl was determined to be 17 % greater than that dissolved in aqueous AcOH (n=2). This is consistent with the CE results (see section 3.4.). PM experiments were also conducted with the solvent as the background electrolyte as is used for TDA (Fig. S5). Chitosan in aqueous HCl had the Cl^- peak superimposed on top of the chitosan peak in these conditions, while it was not the case of the chitosan in aqueous AcOH with the AcO^- migrating earlier. From the PM results it was concluded that aqueous HCl was able to dissolve chitosan to a greater extent than aqueous AcOH.

3.4. Evaluation of dissolution by capillary electrophoresis and pressure-assisted capillary electrophoresis

CE is growing in use for the characterization of macromolecules such as chitosan [22]. CE in the critical conditions has previously been studied to separate polylysine with a degree of polymerization below 10 [42] and chitosan samples by their *DA* [5]. CE in the critical conditions was used in this work to analyze the dissolution of chitosan in different solvents (Fig. 3). All separations were repeatable, but chitosan dissolved in aqueous HCl systematically led to higher recovery in CE. The dissolution of chitosan in aqueous HCl is seen to be more effective than in aqueous AcOH, both at room temperature and at 60°C. The integration of the chitosan peak showed that the chitosan dissolved in aqueous HCl had at least a 13 % greater peak area compared to that dissolved in aqueous AcOH (n=3). The

dissolution in aqueous TFA is as effective as in aqueous HCl at room temperature but at 60 °C it is not (being then comparable to dissolution in aqueous AcOH). These results are consistent with the initial results obtained from the pressure mobilization and it shows that aqueous AcOH is less efficient as a solvent for chitosan than aqueous HCl even though clear suspensions are produced in both cases. To increase the precision of the determination of the mobility, PACE was undertaken. PACE is CE with an added pressure during the separation. This is beneficial as the separation of chitosan takes place in a shorter time and the electroosmotic flow (EOF) is detected. The detection of the EOF allows a more precise determination of the electrophoretic mobilities of chitosan through a double correction with the use of an EOF marker and an electrophoretic mobility marker (Fig. 4). Further, it allows the correction of the area of the chitosan by the hexaamminecobalt(III) chloride internal standard area (to compensate for variations in injection volumes) and the detection of any neutral impurities that could not be seen in CE of chitosan without very long measuring times. The increase in precision is extremely important as any shifts in mobility caused by possible deacetylation (loss of charge) would be noticed during PACE measurements and be more accurately measured. Therefore, experiments monitoring the kinetics of dissolution (see sections 3.6. and 3.7.) with CE were undertaken using PACE.

3.5. Bias in dissolution evaluated with NMR spectroscopy

The measurement of the average degree of acetylation of chitosan is routine in its characterization. Solid-state NMR spectroscopy measurements allow the analysis of the whole sample and an accurate degree of acetylation to be attained. This is further significant taking into account the aforementioned difficulties in obtaining a true solution. A comparison of results from solid-state and solution-state NMR spectroscopy further identifies this bias. The error bars for the solution-state NMR spectroscopy results are based on the relative standard deviation *RSD* estimated from the signal-to-noise ratio *SNR* (Eq. 2 [43]).

$$RSD(\%) = \frac{238}{SNR^{1.28}} \quad (2)$$

The error bars for the solid-state NMR spectroscopy results are based on error caused by phasing and *SNR*. Limited *SNR* may not only result in a limited precision but it can also affect the way the user will phase the spectrum. This is especially true in the case of solid-state NMR spectroscopy in which the signals are generally quite broad. Therefore the error caused by phasing was tested (Table S5). It was measured by having 4 different users phase 8 different experimental data sets. The *DA* was measured and a *RSD* value was obtained for each data set. The *RSD* from phasing was observed to correlate with the *RSD* from *SNR* (Fig. 5A). Therefore, when the *SNR* was less than 50 the *RSD* of *DA* was estimated as a sum of the error from phasing and the error from *SNR* (Eq. 3). The *RSD* was estimated from the *SNR* (Eq. 2) for measurements with a *SNR* greater than 50, for which it was deemed that the error from phasing would be negligible.

$$RSD(\%) = 11 \times \frac{238}{SNR^{1.28}} - 16 \quad (3)$$

The MedMW2 sample (Table 1 and Fig. 5B) has a significantly higher *DA* value when measured with solid-state NMR spectroscopy compared to solution-state NMR spectroscopy which is not the case for the rest of the samples. The error on the average *DA* obtained by solution-state NMR may thus not be systematic. Solution-state NMR measurements can therefore not be calibrated, for example with chitosan samples standardized by solid-state NMR spectroscopy.

The analysis undertaken in solution state shows only the *DA* of the dissolved fraction of the partially dissolved sample which introduces a bias in the determination of the *DA* of the whole sample. The solid-state NMR spectroscopy measurements considered more accurate due to the fact that they measure the whole sample and not just its soluble fraction. For the solution-state NMR spectroscopy the difficulty in dissolving chains with many acetyl groups was previously noted [2] and therefore it is likely chitosan chains with a large *DA* may remain

undissolved and influence the determination of *DA*. The influence may also cause variance in the total amount of D-glucosamine units in solution as a chain with a block of *N*-acetyl-D-glucosamine units that remain out of solution may cause the rest of the chain to remain out of solution. Such an occurrence would be explained by chitosan's precursor chitin, as chitin has a semi-crystalline structure with extended hydrogen bonding [11]. The deacetylation of chitin may cause some chains to have a tendency to blocks of *N*-acetyl-D-glucosamine [3]. These blocks depending on their size may cause these chitosan chains to remain out of solution and cause an incomplete dissolution. This would explain the overestimation (AK Bio D2, D3) of the *DA* values by solution-state NMR spectroscopy. The solution-state measurements may also be influenced by the use of deuterated HCl (DCl) as explored below.

3.6. Kinetics of dissolution monitored by solution-state NMR spectroscopy and PACE

The kinetics of the dissolution was monitored using solution-state NMR spectroscopy, as previously achieved in the case of starch.[44] Before the kinetics measurement, T_1 relaxation time of the chitosan was measured to allow a quantitative measurement. The T_1 relaxation time of the acetyl peak was 1.2 s which was very similar to that of the backbone signal. Chitosan was suspended in 0.8 M DCl in D_2O. Measurements were taken over a 61 h period with a total of 800 measurements and the probe's temperature was controlled at 60 °C during the experiment. From the second measurement the signals assigned to the backbone between 3 and 5 ppm start to be seen (Fig. S6). A signal in the region of the acetyl signal (1.8-2 ppm) is also seen. However, as the measurements progress a second signal is seen in the same region slightly shifted downfield (Fig. S6).

As the kinetics measurement continues this new signal becomes more intense. An integration of this peak shows a steady increase even after the plateau of the chitosan backbone signal intensity is reached (Fig. 6); this signal is therefore assigned to a product of the deacetylation of chitosan [45]. The sharp signal is indicative of a small/mobile group which supports the

hypothesis of deacetylation. The intensity of the signal at 2.2 ppm reduces over time (after 15 h); this signal is thus assigned to the acetyl group of the chitosan. To check the assignment of the signals, chitosan and chitosan spiked with 50 mM AcOH dissolved in 50 mM DCl in D_2O were measured at 60 °C. The signal of the deacetylation product of chitosan was assigned to free AcOH confirming the occurrence of deacetylation (Fig. S7).

The intensity of the chitosan backbone signal is stable after 10 h (Fig. 6A) however, the signal associated with the acetyl peak and the peak associated to the deacetylation increase and decrease over time, respectively. The detection and quantification of the free AcOH allowed the monitoring of the kinetics of the deacetylation (which is not possible using the acetyl group on the chitosan backbone since it is affected by both dissolution and deacetylation simultaneously). The deacetylation was assumed to follow a 2^{nd} order kinetics:[46] S_N2 reaction with a first order in *N*-acetyl-D-glucosamine units (see Equation S-10). This hypothesis was tested using the acetyl peak of the free AcOH (see Fig. 6B and 6C). A linear correlation is observed when the concentration of the *N*-acetyl-D-glucosamine units is determined as the sum of the integrals of the free AcOH and *N*-acetyl-D-glucosamine signals (NG) on the plateau (Fig. 6B). This NG concentration at the plateau $[NG]_\infty$ corresponds to the total concentration of *N*-acetyl-D-glucosamine units that can be dissolved, regardless of whether they are deacetylated or not in solution. When the total concentration of *N*-acetyl-D-glucosamine units is taken as the dissolved fraction of the initial *N*-acetyl-D-glucosamine units (real time value of [NG] on Fig. 6A), a non-linear relationship is seen (Fig. 6C). This result suggests that deacetylation is able to take place as soon as the chitosan is in contact with the solvent. The use of DCl for the dissolution over HCl may cause the dissolution to be slower since the hydrogen bonding that would normally occur in aqueous HCl is stronger than deuterium bonding. Studies have looked into the deacetylation and hydrolysis of chitin and chitosan in concentrated hydrochloric acid [47, 48] with temperatures of 25 and 30 ºC. It was seen that the concentration of the HCl or DCl used and the composition influenced the rate of

hydrolysis and deacetylation [7]. In these conditions, the concentration of HCl (high concentrations) was shown to play a significant role over temperature (only tested 25 and 35 ºC). However, deacetylation was 4 times faster at 35 ºC compared to 25 ºC and 6 M HCl was shown to be the most efficient in hydrolysis [47]. It was further suggested that the formation of a glucofuranosyl oxazolinium ion occurs in concentrated DCl, however this was not noted in our spectra as there was an absence of the corresponding 3 ^{1}H NMR signals at 7 and between 5 and 4.7 ppm. A lower concentration of acid (0.8 M) was used in this work than in previous research and the glucofuranosyl oxazolinium, if present, is below its limit of detection. Further, the low concentration of DCl used in this work would not support hydrolysis over deacetylation as seen previously.

The monitoring was then repeated with 16 times lower concentration of DCl in D_2O (50 mM) to see if the deacetylation still occurred. The rate of dissolution was surprisingly comparable. Deacetylation was once again detected and confirmed, but more limited. Deacetylation was seen to be between 18 and 24 % of the initial DA value (±3.5 on the DA scale). A dissolution experiment was also undertaken with chitosan dissolved for 55 h in 50 mM HCl and DCl in D_2O. The 2 chitosan samples were precipitated and measured with solid-state NMR spectroscopy. Between 14 and 16 % of the initial DA value (± 1.5 on the DA scale) deacetylation was determined after dissolution. The results suggest that the deacetylation and dissolution of chitosan is complex however occurs even at low concentrations of DCl.

This NMR method is not a high-throughput method to monitor dissolution. Measurements of chitosan in 50 mM DCl and HCl were also undertaken on a Magritek Spinsolve benchtop NMR spectrometer to try and detect the deacetylation of chitosan in aqueous HCl. However, the signals of chitosan were unable to be distinctly resolved at the low concentration (1 $g \cdot L^{-1}$) chosen for minimal aggregation (Fig. S8).

To compare the effects of HCl and DCl on the deacetylation of chitosan, PACE was used to run a kinetic measurement at 60 ºC. CE has an advantage over ^{1}H NMR spectroscopy in its

ability to test both DCl and HCl and a shift in the mobility would be an indication of the deacetylation of chitosan. Samples were kept in the sample tray (set at 60 °C) during the course of the kinetic experiment. The PACE results show an insignificant difference in the extent of chitosan dissolution between 50 mM HCl in water and 50 mM DCl in D_2O (Fig. 7, S9). Further, the peak area of both samples does not significantly change over the course of the kinetics after reaching a plateau at 7 h (within experimental error). This is quicker than the 10 h needed for the plateau to be observed in NMR spectroscopy. This might be due to strong intramolecular interactions persisting in the chitosan macromolecules between 7 and 10 h dissolution (this might be related to the tendency towards blocks of *N*-acetyl-D-glucosamine units).

The deacetylation of chitosan at 60 °C in 50 mM DCl in D_2O was detected in solution-state NMR spectroscopy and it was observed to occur almost immediately. This should correspond in PACE to a shift to higher electrophoretic mobility because of the higher charge [5] as well as a decrease in peak area since the main chromophore of the chitosan should be the acetamide functional group. However, the evidence of deacetylation was not detected in the PACE results: the electrophoretic mobility remains constant throughout the dissolution apart from the first 5 h in which aggregation affects the dissolution and the peak area of the chitosan dissolved in both aqueous solvents remained constant after reaching a plateau after 7 h (Fig. 7). In both cases, the dissolution as well as the deacetylation contribute: some low DA chitosan chains may dissolve a lot quicker than the high DA ones (before the first measurement). The dissolution may thus lead to a shift to lower mobility during the dissolution and this may counterbalance the shift to higher mobility due to deacetylation. A similar effect would be observed on peak area. The absence of mixing of the sample in PACE compared to the rotation of the NMR tube might lead to a lower difference in rate of deacetylation in both systems, but this was not observed in the case of the dissolution. It can be hypothesized through the comparison of the NMR and CE results that higher DA chitosan

chains dissolve quicker and that, at least in DCl, deacetylation of chitosan takes place at a similar rate as the dissolution.

This finding is extremely significant as solution-state NMR spectroscopy is used routinely for the molecular characterization of chitosan especially for *DA* measurements (Table S4). These measurements often use DCl as the methyl from any residual CHD_3COOD in CD_3COOD is likely to overlap with that of the chitosan. DCl causes both degradation and therefore inaccurate measurements are obtained. Conditions used for the solution-state NMR results obtained previously [5] are unlikely to have caused a strong deacetylation due to the short period at higher temperatures; however, the sample would not have been completely dissolved during the measurement and therefore a bias on the measurement of *DA* is clear. Further research is required on obtaining of a "true solution", however it can be concluded that solution-state NMR spectroscopy using 50 mM DCl in D_2O as a solvent yields inaccurate *DA* values.

The effect of acid on the hydrodynamic volume of chitosan was also investigated and compared in the literature [49]. It was concluded that AcOH caused acid hydrolysis when compared to malic acid through a measurement of intrinsic viscosity. This may, however, also be due to a more complete dissolution taking place when compared to malic acid as results undertaken in this study express that chitosan is complicated to dissolve even in aqueous solvents.

3.7. Comparison of the kinetics of dissolution of different chitosan samples

The dissolution of 3 different chitosan samples (MedMW1, LowMW1, HighMW) in 50 mM HCl were analyzed with PACE to compare the effect of molar mass and of *DA* on dissolution. The samples were prepared after the preconditioning of the capillary to obtain an accurate data point at the beginning of the kinetics (t_0). It was seen that the area of the peak for LowMW1, MedMW1 and HighMW reached a plateau (within experimental error) after 7.5 h

(from the 3rd measurement, Fig. 8, S9-11). The peak area was corrected by the average *DA* obtained from the solid-state NMR spectroscopy measurements. The t_0 measurement of HighMW and LowMW1 had a very large signal at the same electrophoretic mobility as chitosan (Fig. S12). This was due to non-repeatable aggregates causing light scattering which would explain the immense absorbance. The dissolution of all 3 samples followed a similar kinetics reaching a plateau after 5 h. The samples dissolution seems to behave similarly with the exception of the t_0 of the HighMW and the LowMW1 which undergoes aggregation. The LowMW1 and MedMW1 are notably less soluble in aqueous HCl than the HighMW with approximately 35 % difference in the peak area (n=2). Low or medium molar masses are expected to lead to faster and potentially more complete dissolution than higher molar masses. It should be noted that the molar masses are of limited accuracy notably due to aggregation (as see with SEC in this work) and incomplete dissolution or deacetylation. Therefore the molar mass supplied may not be representative of the sample. More importantly, HighMW has the lowest average *DA*. A lower *DA* is known to lead to faster and more complete dissolution. Assuming the relative difference of molar mass of the three chitosan samples is true, the results signify *DA* has a greater role in dissolution than molar mass.

4. Conclusions

Through this study we have showed that the dissolution of chitosan is quite challenging and often overlooked. The presence of aggregates even at low concentrations of chitosan complicates the dissolution and prevents from obtaining a true solution. However, this study was able to show that aqueous AcOH was less efficient at dissolving chitosan when compared to aqueous HCl and the dissolution in aqueous TFA is as efficient only at room temperature. This information is significant due to the prominent use of AcOH in the dissolution of chitosan for various applications, as well as characterization methods such as SEC for molar mass calculations or CE for the separation of chitosan by its *DA*. Several studies characterize

the average *DA* or the molar mass of chitosan on the assumption that all the chains of chitosan are dissolved and the result obtained is representative of the whole sample [11]. A study undertaken to analyze the *DA* of chitosan and its distribution by SEC concluded that the characterization in solution may have been impeded by artifacts [50]. These artifacts could, however, have been the presence of aggregates due to the use of AcOH as a solvent as identified in a later study [18]. Due to the presence of aggregates and the inability to remove them from the solution, it was concluded that characterization was only possible for a small number of samples. The SEC results obtained in our study further supports the presence of aggregation through the extremely large molar mass values determined. The kinetics measurements gave further information regarding the behavior of chitosan in solution and showed the increase in deacetylation caused by long periods at high temperature as well as partial deacetylation in shorter time periods. Samples with different *DA*s measured by NMR spectroscopy were successfully studied and the effects of *DA* on the dissolution were compared by PACE. The average *DA* may play a more important role in the completeness of dissolution than the molar mass. Further, time-resolved NMR spectroscopy and PACE showed that 50 mM DCl is an inappropriate solvent for chitosan due to deacetylation. Following these results, previous measurements of the average *DA* of chitosan in 50 mM DCl using solution-state NMR spectroscopy (Table S4), including from our team [5] should be considered very carefully and rather replaced with values obtained by solid-state NMR spectroscopy as published by others [27, 28] and as obtained in this work. Future work should focus on improving the solubility while minimizing the degradation and this may involve the use of salts as a hydrogen bond disruptor as in the cases of cellulose [51] and starch [8] or the use of ionic liquids [52]. The stability of chitosan in simulated gastric fluid (SGF) and simulated intestinal fluid (SIF) could also be analyzed to help assess the use of chitosan as a drug delivery agent.

Acknowledgements

JJT thanks Matthew Van Leeuwen (WSU) for assistance in the lab, Alison Maniego (WSU), Michelle Toutounji (WSU) and Lucie Seiler (University Paul Sabatier, Toulouse, France) for assistance with NMR spectroscopy data treatment, and the Australian Government for the Endeavour Research Fellowship to travel to the Max Planck Institute for Polymer Research, Mainz, Germany. MG and PC thank the Molecular Medicine Research Group at WSU for Research Seed Funding. We thank Robert Graf (MPIP), Michael O'Connor (WSU) and Richard Wuhrer (AMCF, WSU) for insightful discussions, Malvern Instruments and ATA Scientific, especially Bryn McDonagh, for the loan of a Triple Detector Array SEC, as well as and Magritek, especially Mitchell Goshert, Peter Hulmston and Andrew Coy, for the loan of a benchtop NMR spectrometer.

References

[1] S. Trombotto, C. Ladaviere, F. Delolme, A. Domard, Chemical preparation and structural characterization of a homogeneous series of chitin/chitosan oligomers, Biomacromolecules, 9 (2008) 1731-1738.
[2] M. Rinaudo, Chitin and chitosan: Properties and applications, Prog. Polym. Sci., 31 (2006) 603-632.
[3] A. Domard, A perspective on 30 years research on chitin and chitosan, Carbohydr. Polym., 84 (2011) 696-703.
[4] Z. Li, M. Leung, R. Hopper, R. Ellenbogen, M. Zhang, Feeder-free self-renewal of human embryonic stem cells in 3D porous natural polymer scaffolds, Biomaterials, 31 (2010) 404-412.
[5] M. Mnatsakanyan, J.J. Thevarajah, R.S. Roi, A. Lauto, M. Gaborieau, P. Castignolles, Separation of chitosan by degree of acetylation using simple free solution capillary electrophoresis, Anal. Bioanal. Chem., 405 (2013) 6873-6877.
[6] G. Lamarque, C. Viton, A. Domard, Comparative study of the first heterogeneous deacetylation of alpha- and beta-chitins in a multistep process, Biomacromolecules, 5 (2004) 992-1001.
[7] A. Einbu, K.M. Varum, Characterization of chitin and its hydrolysis to GlcNAc and GlcN, Biomacromolecules, 9 (2008) 1870-1875.
[8] S. Schmitz, A.C. Dona, P. Castignolles, R.G. Gilbert, M. Gaborieau, Assessment of the Extent of Starch Dissolution in Dimethyl Sulfoxide by 1H NMR Spectroscopy, Macromol. Biosci., 9 (2009) 506-514.
[9] B.A. Miller-Chou, J.L. Koenig, A review of polymer dissolution, Prog. Polym. Sci., 28 (2003) 1223-1270.

[10] C. Lefay, Y. Guillaneuf, G. Moreira, J.J. Thevarajah, P. Castignolles, F. Ziarelli, E. Bloch, M. Major, L. Charles, M. Gaborieau, D. Bertin, D. Gigmes, Heterogeneous modification of chitosan via nitroxide-mediated polymerization, 4 (2013) 322-328.
[11] C.K.S. Pillai, W. Paul, C.P. Sharma, Chitin and chitosan polymers: Chemistry, solubility and fiber formation, Prog. Polym. Sci., 34 (2009) 641-678.
[12] Y.I. Jeong, D.G. Kim, M.K. Jang, J.W. Nah, Preparation and spectroscopic characterization of methoxy poly(ethylene glycol)-grafted water-soluble chitosan, Carbohydr. Res., 343 (2008) 282-289.
[13] T.P. Kravtchenko, J. Renoir, A. Parker, G. Brigand, A novel method for determining the dissolution kinetics of hydrocolloid powders, 13 (1999) 219-225.
[14] Y. Zhang, S.K. Mallapragada, B. Narasimhan, A Novel High Throughput Method to Investigate Polymer Dissolution, 31 (2010) 385-390.
[15] A. Chojnacka, H.G. Janssen, P. Schoenmakers, Detailed study of polystyrene solubility using pyrolysis-gas chromatography-mass spectrometry and combination with size-exclusion chromatography, Anal. Bioanal. Chem., 406 (2014) 459-465.
[16] A. Chojnacka, A. Ghaffar, A. Feilden, K. Treacher, H.G. Janssen, P. Schoenmakers, Pyrolysis-gas chromatography-mass spectrometry for studying N-vinyl-2-pyrrolidone-co-vinyl acetate copolymers and their dissolution behaviour, Anal. Chim. Acta, 706 (2011) 305-311.
[17] M.W. Anthonsen, K.M. Varum, A.M. Hermansson, O. Smidsrod, D.A. Brant, Aggregates in Acidic Solutions of Chitosans detected by static Laser-Light Scattering, Carbohydr Polym., 25 (1994) 13-23.
[18] M. Yanagisawa, Y. Kato, Y. Yoshida, A. Isogai, SEC-MALS study on aggregates of chitosan molecules in aqueous solvents: Influence of residual N-acetyl groups, Carbohydr. Polym., 66 (2006) 192-198.
[19] M. Gaborieau, P. Castignolles, Size-exclusion chromatography (SEC) of branched polymers and polysaccharides, Anal. Bioanal. Chem., 399 (2011) 1413-1423.
[20] M.H. Ottoy, K.M. Varum, B.E. Christensen, M.W. Anthonsen, O. Smidsrod, Preparative and analytical size-exclusion chromatography of chitosans, Carbohydr. Polym., 31 (1996) 253-261.
[21] T. Le Saux, H. Cottet, Size-based characterization by the coupling of capillary electrophoresis to Taylor dispersion analysis, Anal. Chem., 80 (2008) 1829-1832.
[22] J.J. Thevarajah, M. Gaborieau, P. Castignolles, Separation and characterization of synthetic polyelectrolytes and polysaccharides with capillary electrophoresis, 2014 (2014) Article ID 798403.
[23] D.L. Taylor, C.J. Ferris, A.R. Maniego, P. Castignolles, M. in het Panhuis, M. Gaborieau, Characterization of Gellan Gum by Capillary Electrophoresis, 65 (2012) 1156-1164.
[24] M. Gaborieau, T. Causon, Y. Guillaneuf, E.F. Hilder, P. Castignolles, Molecular weight and tacticty of oligoacrylates by capillary electrophoresis - mass spectrometry, Aus. J. Chem., 63 (2010) 1219-1226.
[25] J.J. Thevarajah, A.T. Sutton, A.R. Maniego, E.G. Whitty, S. Harrisson, H. Cottet, P. Castignolles, M. Gaborieau, Quantifying the Heterogeneity of Chemical Structures in Complex Charged Polymers through the Dispersity of Their Distributions of Electrophoretic Mobilities or of Compositions, Anal. Chem., 88 (2016) 1674-1681.
[26] J. Chamieh, M. Martin, H. Cottet, Quantitative Analysis in Capillary Electrophoresis: Transformation of Raw Electropherograms into Continuous Distributions, Anal. Chem., 87 (2015) 1050-1057.
[27] M.H. Ottoy, K.M. Varum, O. Smidsrod, Compositional heterogeneity of heterogeneously deacetylated chitosans, Carbohydr. Polym., 29 (1996) 17-24.

[28] L. Heux, J. Brugnerotto, J. Desbrieres, M.F. Versali, M. Rinaudo, Solid state NMR for determination of degree of acetylation of chitin and chitosan, Biomacromolecules, 1 (2000) 746-751.
[29] C.R. Morcombe, K.W. Zilm, Chemical shift referencing in MAS solid state NMR, J. Magn. Reson., 162 (2003) 479-486.
[30] R. Novoa-Carballal, E. Fernandez-Megia, R. Riguera, Dynamics of Chitosan by H-1 NMR Relaxation, Biomacromolecules, 11 (2010) 2079-2086.
[31] C. Prego, D. Torres, E. Fernandez-Megia, R. Novoa-Carballal, E. Quinoa, M.J. Alonso, Chitosan-PEG nanocapsules as new carriers for oral peptide delivery - Effect of chitosan pegylation degree, J. Control. Release, 111 (2006) 299-308.
[32] E. Fernandez-Megia, R. Novoa-Carballal, E. Quiñoá, R. Riguera, Optimal routine conditions for the determination of the degree of acetylation of chitosan by 1H-NMR, Carbohydr. Polym., 61 (2005) 155-161.
[33] M. de la Fuente, B. Seijo, M.J. Alonso, Bioadhesive hyaluronan-chitosan nanoparticles can transport genes across the ocular mucosa and transfect ocular tissue, Gene Ther., 15 (2008) 668-676.
[34] Polymer Standards Service, Characterization of Chitin/Chitosan, GPC/SEC application note 10280.
[35] D. Berek, Size exclusion chromatography - A blessing and a curse of science and technology of synthetic polymers, J. Sep. Sci., 33 (2010) 315-335.
[36] D. Muller, M. Ndoumenze, J. Jozefonvicz, High-pressure size-exclusion chromatography of anticoagulant materials, J. Chromatogr., 297 (1984) 351-358.
[37] Y. Guillaneuf, P. Castignolles, Using apparent Molecular Weight from SEC in controlled/living polymerization and kinetics of polymerization, J. Polym. Sci. A Polym. Chem., 46 (2008) 897-911.
[38] M. Gaborieau, J. Nicolas, M. Save, B. Charleux, J.-P. Vairon, R.G. Gilbert, P. Castignolles, Multiple-detection size-exclusion chromatography of complex branched polyacrylates, J. Chromatogr. A, 1190 (2008) 215-233.
[39] W. Praznik, A. Huber, De facto molecular weight distributions of glucans by size-exclusion chromatography combined with mass/molar-detection of fluorescence labeled terminal hemiacetals, J. Chromatogr. B, 824 (2005) 295-307.
[40] L.T. Cherney, A.P. Petrov, S.N. Krylov, One-Dimensional Approach to Study Kinetics of Reversible Binding of Protein on Capillary Walls, Anal. Chem., 87 (2015) 1219-1225.
[41] N. Higashi, Y. Ozaki, Potential of far-ultraviolet absorption spectroscopy as a highly sensitive quantitative and qualitative analysis method for aqueous solutions, Part I: Determination of hydrogen chloride in aqueous solutions, Appl. Spectrosc., 58 (2004) 910-916.
[42] H.F. Wu, S.A. Allison, C. Perrin, H. Cottet, Modeling the electrophoresis of highly charged peptides: Application to oligolysines, J. Sep. Sci., 35 (2012) 556-562.
[43] P. Castignolles, R. Graf, M. Parkinson, M. Wilhelm, M. Gaborieau, Detection and quantification of branching in polyacrylates by size-exclusion chromatography (SEC) and melt-state 13C NMR spectroscopy, Polymer, 50 (2009) 2373-2383.
[44] A. Dona, C.-W.W. Yuen, J. Peate, R.G. Gilbert, P. Castignolles, M. Gaborieau, A new NMR method for directly monitoring and quantifying the dissolution kinetics of starch in DMSO, Carbohydr. Res., 342 (2007) 2604-2610.
[45] M. Lavertu, Z. Xia, A.N. Serreqi, M. Berrada, A. Rodrigues, D. Wang, M.D. Buschmann, A. Gupta, A validated 1H NMR method for the determination of the degree of deacetylation of chitosan, J. Pharma. Biomed. Anal., 32 (2003) 1149-1158.
[46] K.M. Varum, M.H. Ottoy, O. Smidsrod, Acid hydrolysis of chitosans, Carbohydr. Polym., 46 (2001) 89-98.

[47] A. Einbu, K.M. Varum, Depolymerization and de-N-acetylation of chitin oligomers in hydrochloric acid, Biomacromolecules, 8 (2007) 309-314.
[48] A. Einbu, H. Grasdalen, K.M. Varum, Kinetics of hydrolysis of chitin/chitosan oligomers in concentrated hydrochloric acid, Carbohydr. Res., 342 (2007) 1055-1062.
[49] R.H. Chen, W.Y. Chen, S.T. Wang, C.H. Hsu, M.L. Tsai, Changes in the Mark-Houwink hydrodynamic volume of chitosan molecules in solutions of different organic acids, at different temperatures and ionic strengths, Carbohydr. Polym., 78 (2009) 902-907.
[50] G. Berth, H. Dautzenberg, The degree of acetylation of chitosans and its effect on the chain conformation in aqueous solution, Carbohydr. Polym., 47 (2002) 39-51.
[51] M. Kostag, T. Liebert, T. Heinze, Acetone-Based Cellulose Solvent, Macromol. Rapid Commun., 35 (2014) 1419-1422.
[52] M. Gericke, P. Fardim, T. Heinze, Ionic Liquids - Promising but Challenging Solvents for Homogeneous Derivatization of Cellulose, Molecules, 17 (2012) 7458-7502.

Table 1. Visual evaluation of the dissolution of chitosan samples with varied *DA*s in aqueous solvents: 50 mM HCl, 0.3 % (w/v) trifluoroacetic acid (TFA), as well as 0.3 % (w/v) TFA with 0.1 M NaCl (Eluent)

Sample	Supplier	Batch (Catalogue)	$DA_n^{SS\text{-}NMR}$ (%) [a]	DA_n^{NMR} (%)[b]	HCl	TFA	Eluent
LowMW1	Sigma	MKBG3334V (448869)	17.1 ± 0.3		2h[c]	2h	2h
MedMW1	Sigma	MKBH1108V (448877)	22.3 ± 0.3		2h	2h	1n [d]
MedMW2	Sigma	03318AJ (448877)	20.2 ± 0.3	15.5 ± 1.6	1n	1n	
HighMW	Sigma	MKBD7240V (419419)	11.8 ± 0.3		1n	1n	
Sig	Sigma	120M0028V (C3646)	10.1 ± 0.3		1n	1n	
AKbioV1	AK Biotech	090426V1	10.1 ± 0.3		1n	1n	
AKbioV2	AK Biotech	090423V2	16.5 ± 0.3	18.7 ± 1.9	1n	1n	
AKbioV3	AK Biotech	090426V3	14.8 ± 0.3	16.5 ± 1.7	1n	1n	
AKbioD1	AK Biotech	090422D1	12.5 ± 0.3	19.8 ± 2.0	1n	1n	
AKbioD2	AK Biotech	090422D2	11.1 ± 0.3	13.6 ± 1.4	1n	1n	
AKbioD3	AK Biotech	090422D3	3.8 ± 0.3	3.5 ± 0.4	1n	1n	
AKbioC	AK Biotech	090430C			2w[e]	2w	
ChitAl	[5]		4.0 ± 0.3	2.5 ± 0.3	2h		

[a] Number-average *DA* obtained by solid-state NMR spectroscopy in this work for which the *SD* was determined as the error caused by phasing (see section 3.5.)

[b] Number-average *DA* obtained by solution-state NMR spectroscopy [5]

[c] sample was visually dissolved after 2 h at 60 °C

[d] sample was visually dissolved after 2 h at 60 °C and an overnight shaking at room temperature

[e] sample was visually dissolved after 2 h at 60 °C followed by overnight shaking at room temperature followed by 2 weeks without shaking at room temperature

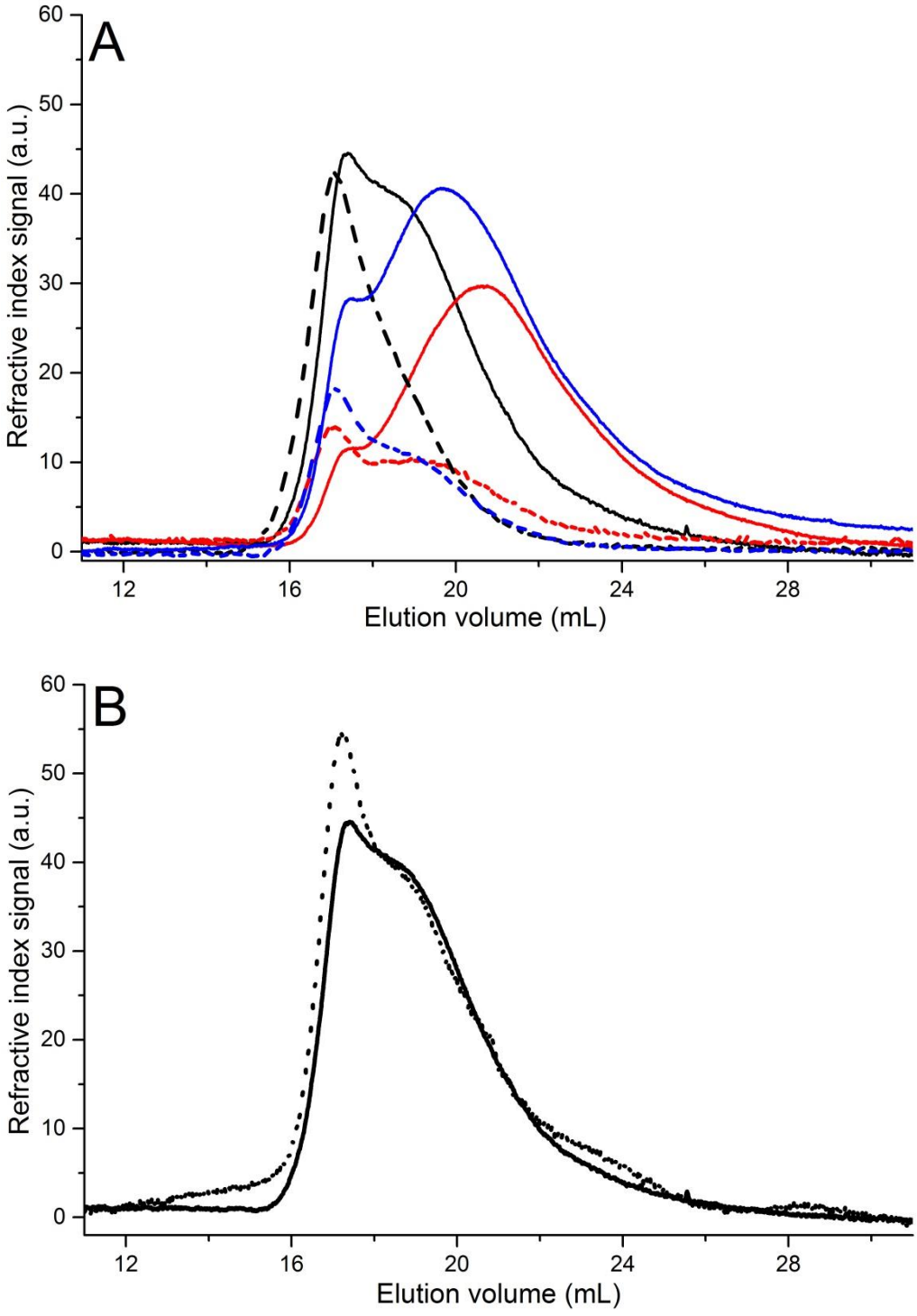

Figure 1: A) RI (solid lines) and RALS (dashed lines) traces of chitosan MedMW1 (black), LowMW1 (red) and AKbioD3 (blue). B) RI trace of MedMW1 in 50 mM HCl at 1 $g \cdot L^{-1}$ (solid line) and diluted to 0.25 $g \cdot L^{-1}$ (normalized by concentration, dotted line)

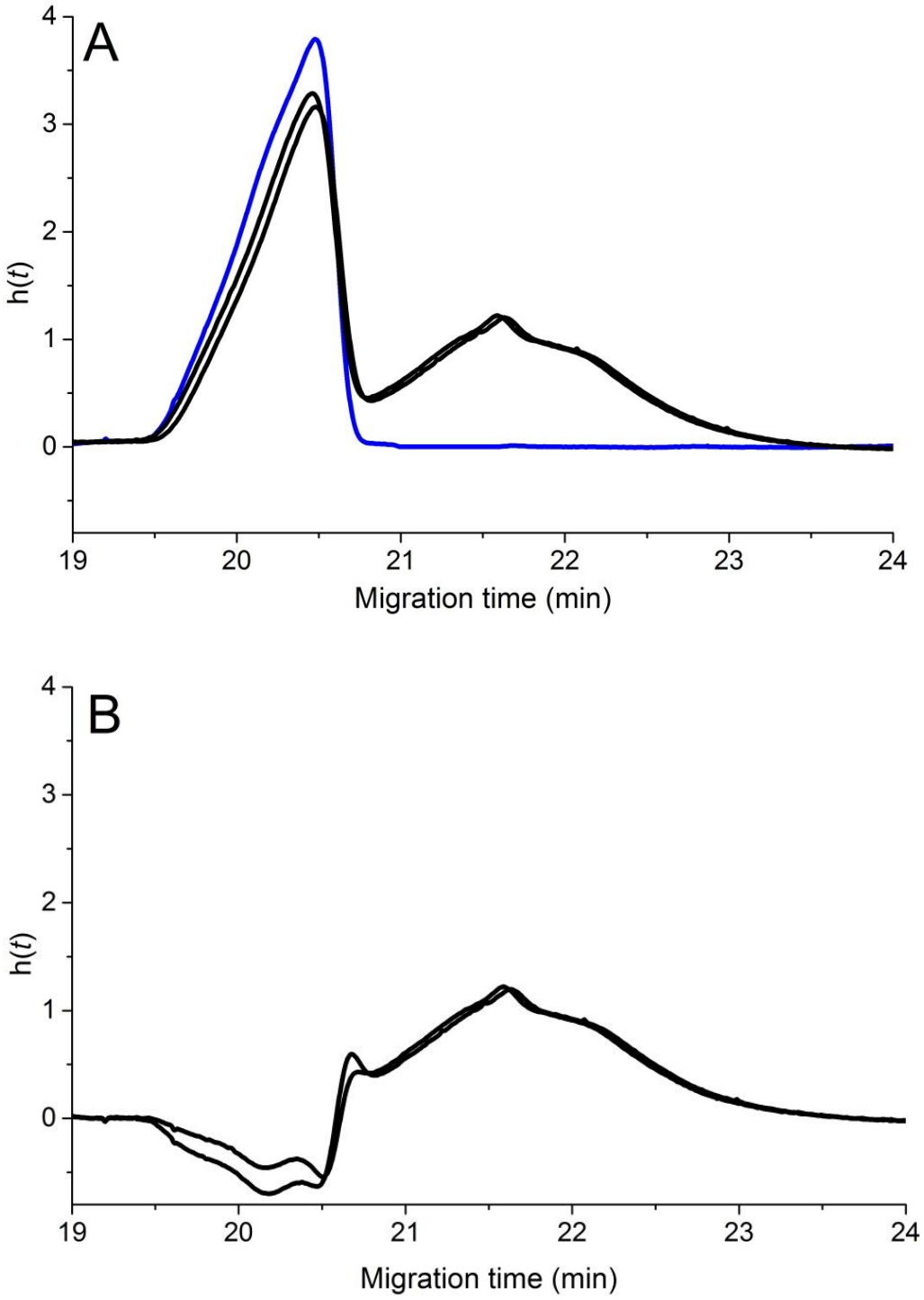

Figure 2: PM (with viscosity normalization for Cl^-) of 50 mM HCl (blue) and of chitosan (MedMW1) dissolved in 50 mM HCl (black, 2 repeat experiments shown) A) before and B) after Cl^- subtraction

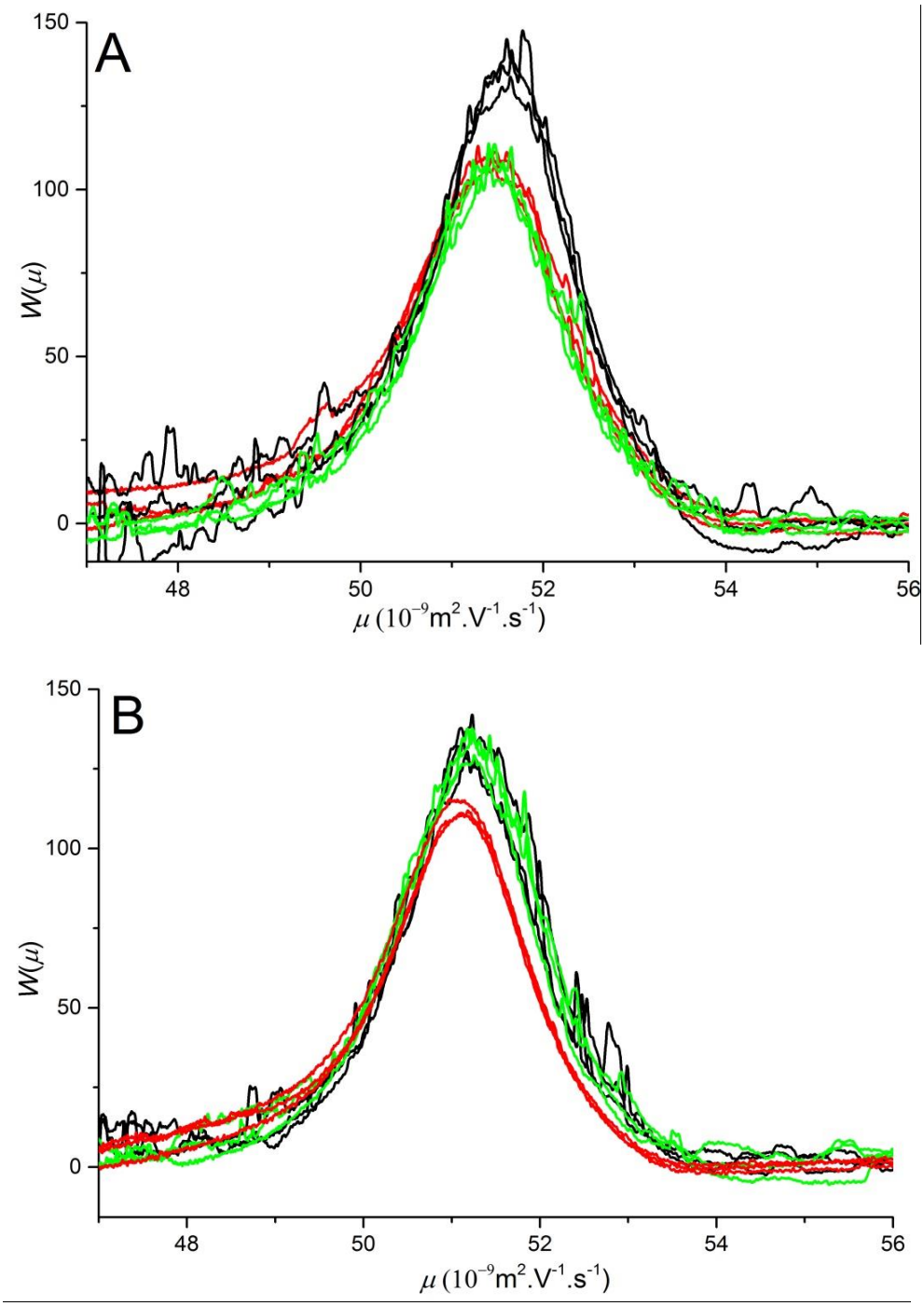

Figure 3: Electropherogram of chitosan (MedMW1) dissolved in 50 mM HCl (black line), AcOH (red line) and TFA (green line) prepared at A) 60 °C for 2 h B) 25 °C for 2 h

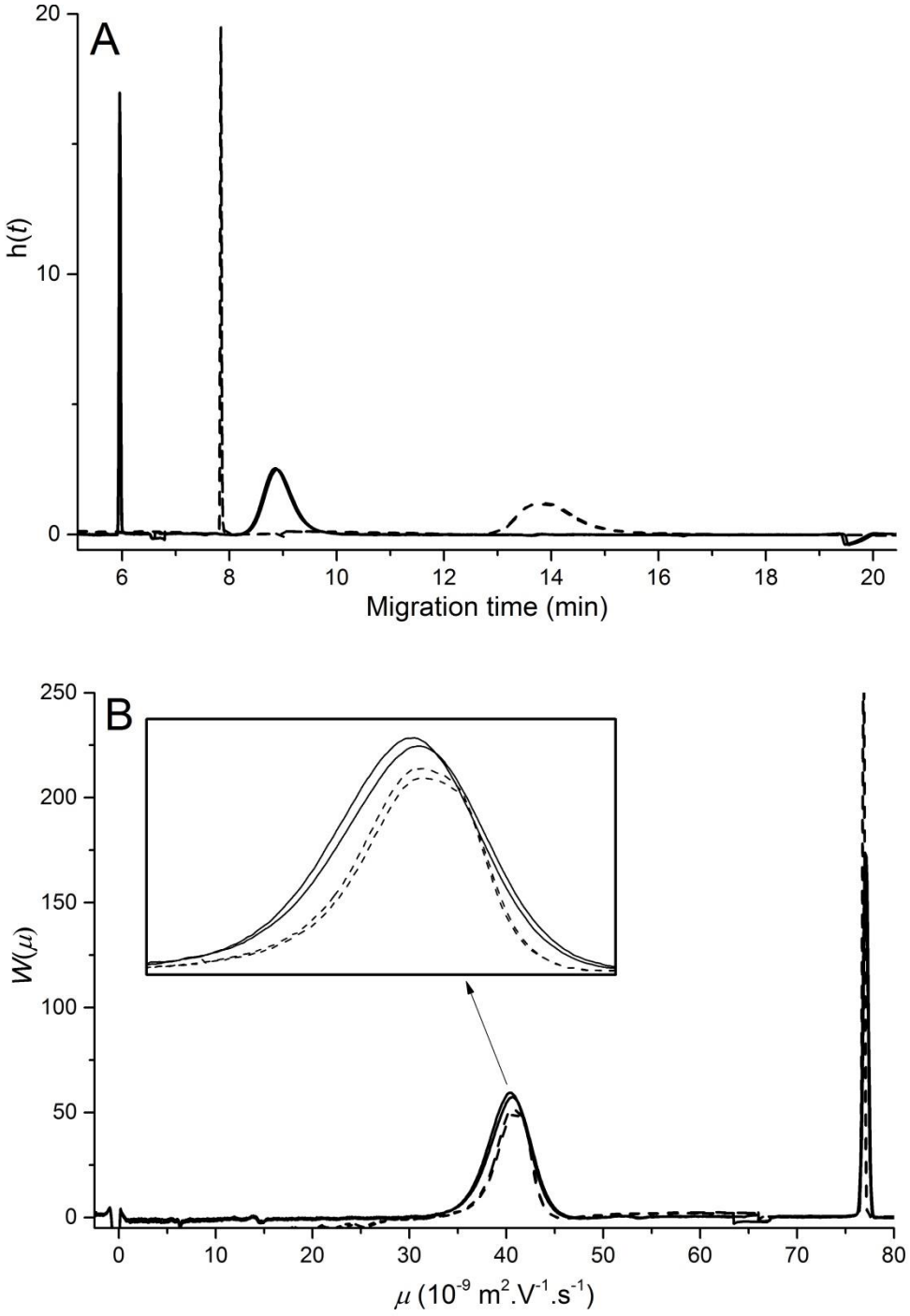

Figure 4. Electropherogram of chitosan (MedMW1) dissolved in 50 mM HCl separated using CE (dashed line) and PACE (solid line) in a) migration time and b) electrophoretic mobility. The electrophoretic mobility marker is seen at a mobility of 76.9×10^{-9} $m^2.V^{-1}.s^{-1}$ and a migration time between 6 and 8 min. The EOF is seen at a mobility of 0.

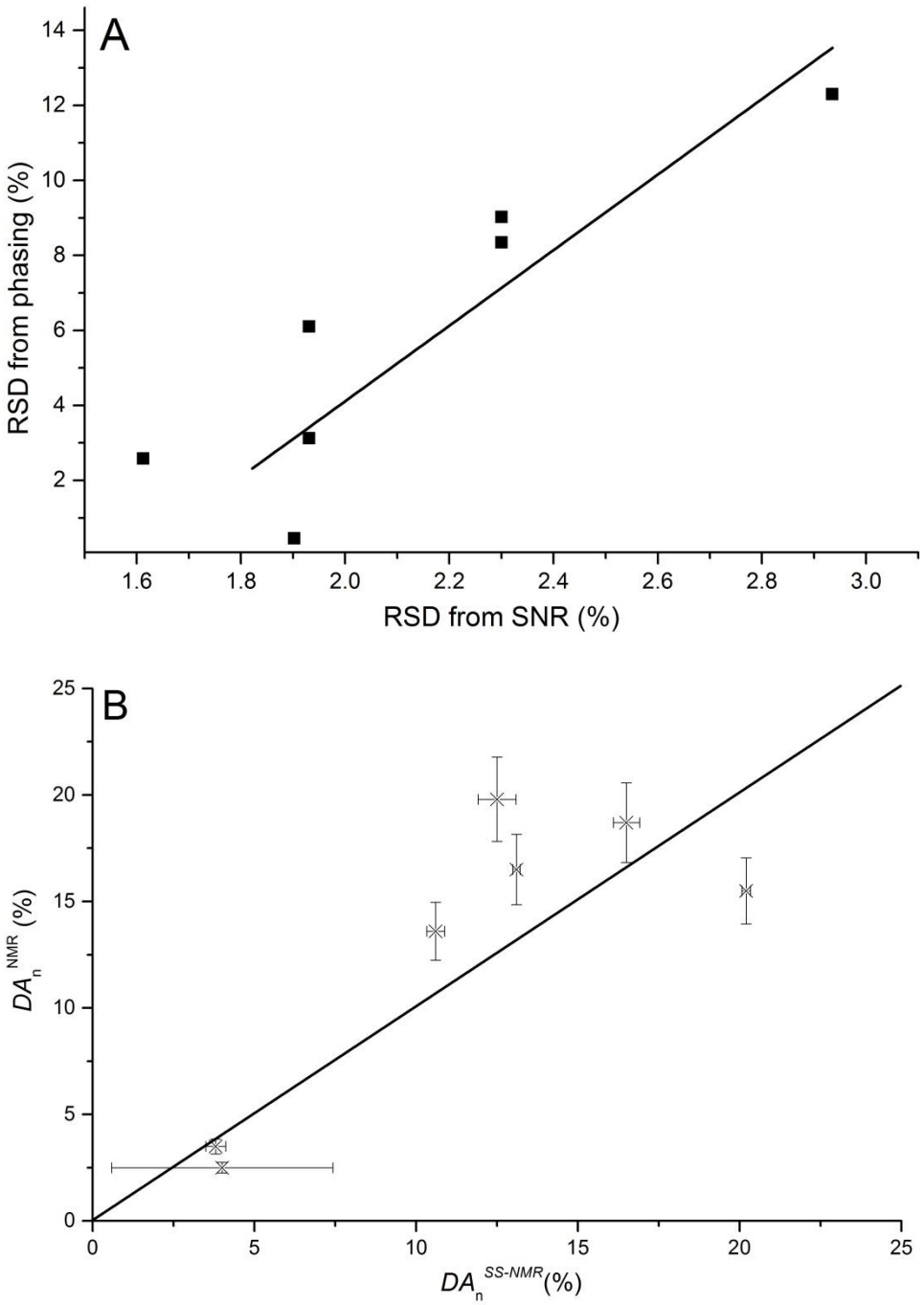

Figure 5: A. Error of solid-state NMR spectroscopy measurements estimated as *RSD* from *SNR* and as *RSD* from phasing. The straight line represents a linear fit (y=10x-16, R^2=0.79). B. *DA* values obtained by solution- and solid-state NMR spectroscopy for the same chitosan samples. The straight line is the diagonal.

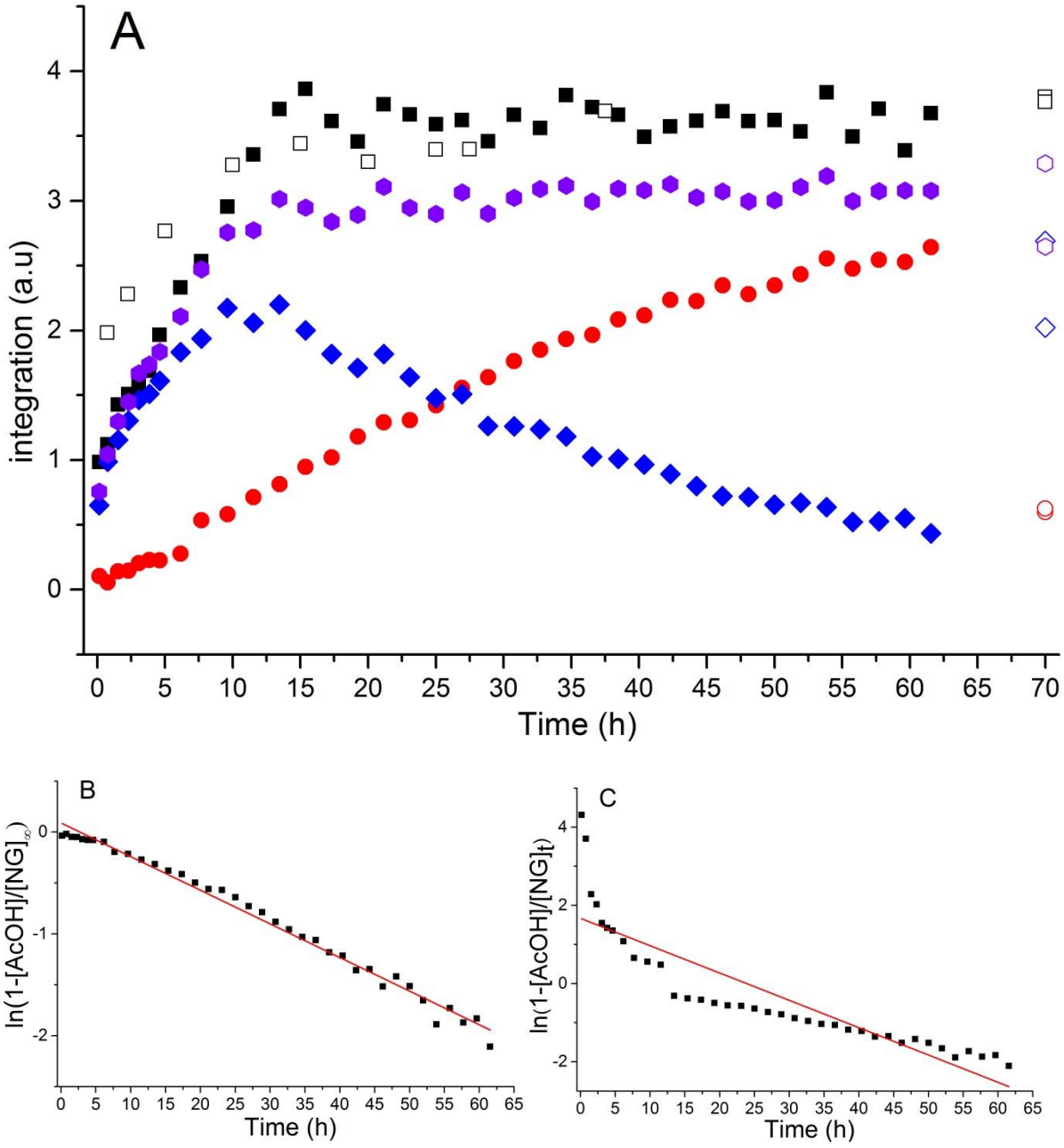

Figure 6. A. Integration of solution-state NMR signals measured over 61 h at 60 °C: chitosan backbone (black squares), chitosan acetyl group (blue diamonds), free AcOH (red circles) and the sum of the acetyl group and free AcOH (NG, purple hexagons). The full symbols correspond to measurements in 0.8 M DCl in D_2O, the empty symbols to measurements in 50 mM in D_2O.. Evolution on a logarithmic scale of the consumption of the acetyl groups on *N*-acetyl-D-glucosamine units, with the *N*-acetyl-D-glucosamine concentration taken as (B) the total available initial *N*-acetyl-D-glucosamine units $[NG]_\infty$ (plateau of NG purple curve in A)

or (C) as the dissolved fraction of the initial *N*-acetyl glucosamine units $[NG]_t$ (real time value of NG purple curve in A). Red lines represent linear fits with a r^2 of 0.99 (B) and 0.77 (C).

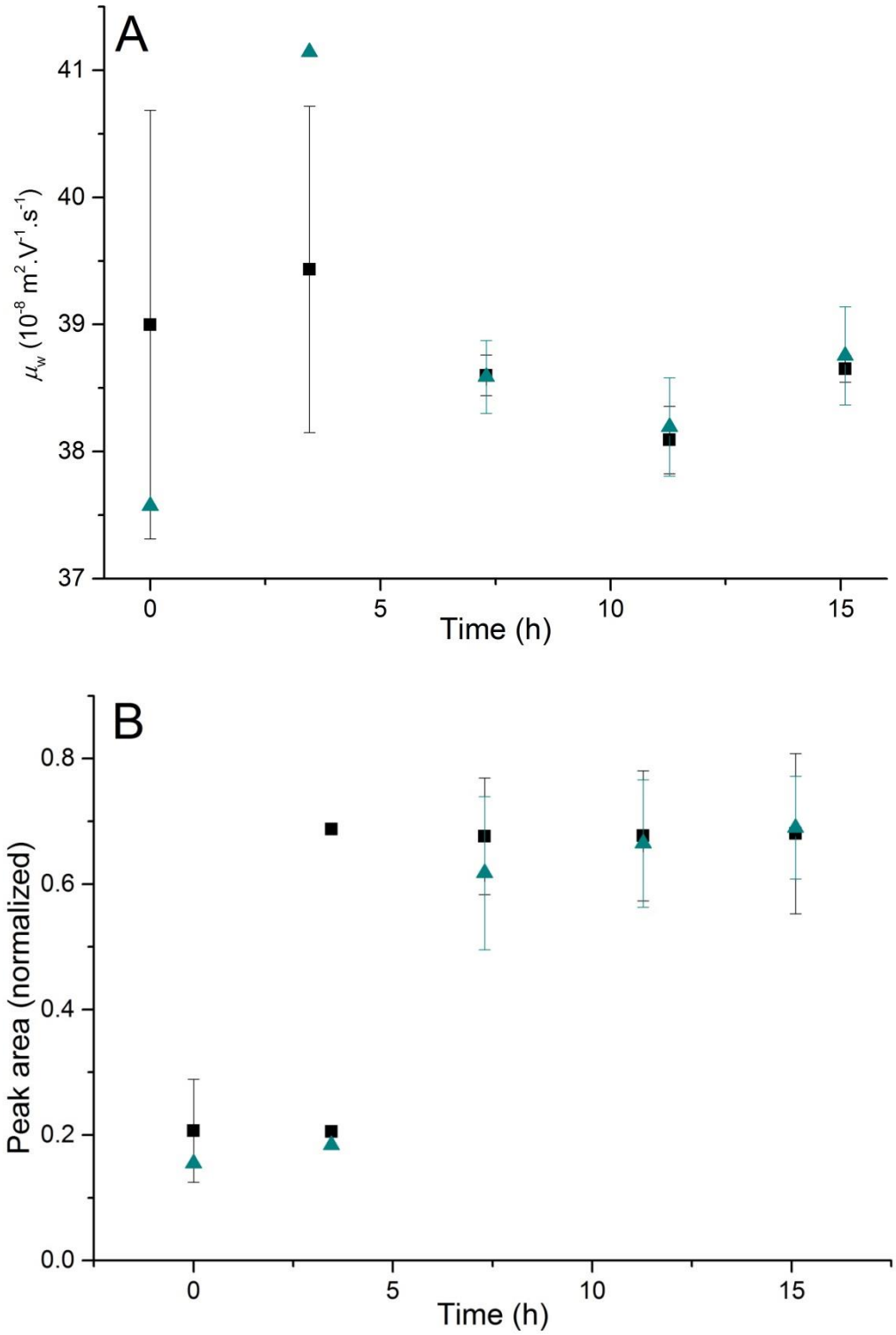

Figure 7. A. Weight-average mobility μ_w and B. Integral of chitosan peak in kinetics of dissolution monitored with PACE in 50 mM HCl in water (black squares) and DCl in D_2O (green triangles).

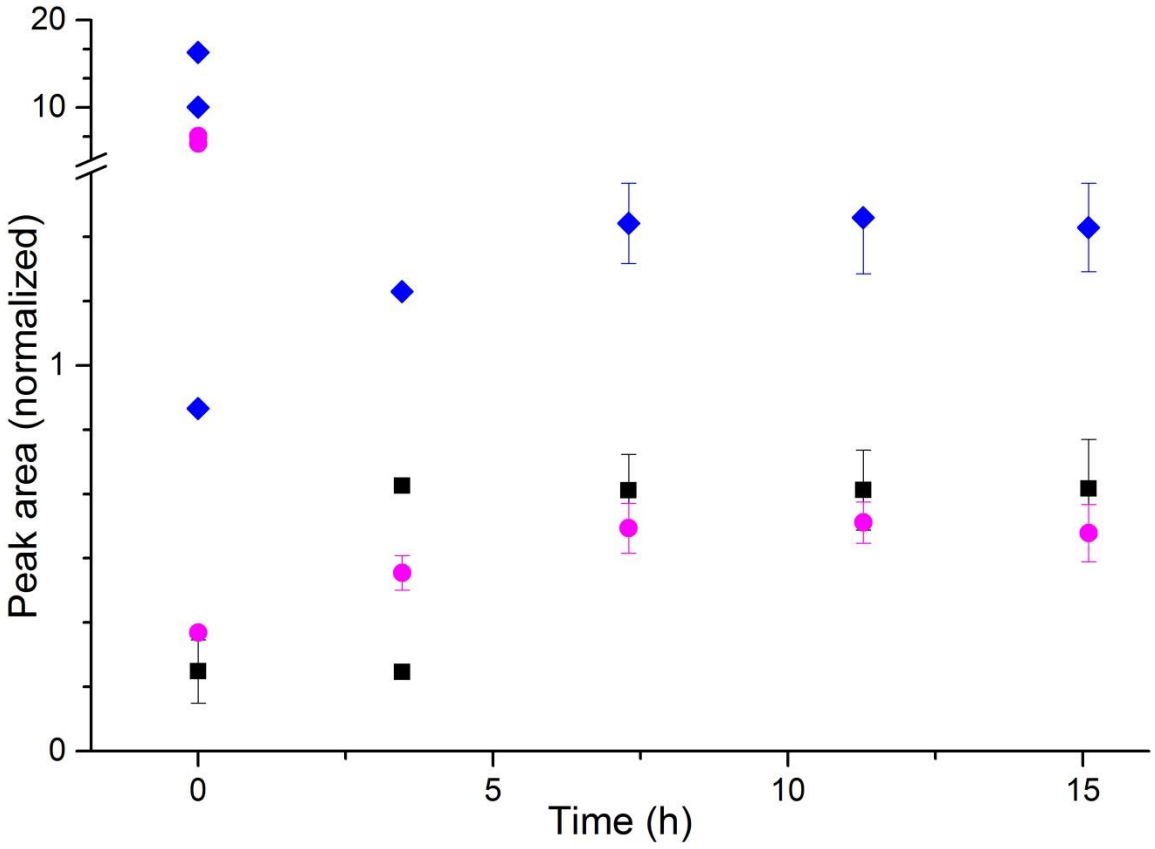

Figure 8. Integration of the peak area in a kinetics of dissolution of MedMW1 (black squares), LowMW1 (magenta circles) and HighMW (blue diamonds) chitosan undertaken with PACE in 50 mM HCl (n=2).

Supporting information
For
Towards a less biased dissolution of chitosan

Joel J. Thevarajah [a,b,c], Jerikho C. Bulanadi [a], Manfred Wagner [c], Marianne Gaborieau [a,b]*, Patrice Castignolles [a]

[a] Western Sydney University, School of Science and Health, Australian Centre for Research on Separation Sciences (ACROSS), Parramatta, 2150, Australia

[b] Western Sydney University, Molecular Medicine Research Group (MMRG), School of Science and Health, Parramatta, 2150, Australia [c] Max Planck Institute for Polymer Research, 55128 Mainz, Ackermannweg 10, Germany

*Corresponding author : Marianne Gaborieau, m.gaborieau@westernsydney.edu.au

Visual observation of dissolution

A range of aqueous acids were chosen at different concentrations to assess the dissolution of chitosan at room temperature, 40 °C and 60 °C (see Tables S1 and S2).

Table S1: Visual evaluation of MedMW2 chitosan dissolution in various aqueous acids and sodium borate buffer at room temperature. "Yes" indicates transparency within 15 minutes.

	Concentration				
Acid	5 mM	10 mM	50 mM	1 % [a)]	5 % [a)]
Hydrochloric	No	No	Yes	Yes	-
Acetic	No	No	Yes	Yes	-
Trifluoroacetic	No	No	Yes	Yes	-
Phosphoric	-	-	No	No	No
Boric	-	-	No	No	No
Borate Buffer	-	-	No	-	-
Trifluoroacetic acid (0.3%) [a)]	-	-	No	-	-

- indicates that the experiment was not conducted

[a)] Unit was % w/v for boric acid and % v/v for the others

Table S2: Visual evaluation of MedMW2 chitosan dissolution at higher temperatures in various aqueous acids and sodium borate buffer. “Yes” indicates transparency after 1 hour.

Temperature	40 °C		60 °C	
Concentration	50 mM	1 %	50 mM	1 %
Phosphoric acid	Partial	Partial	Yes	Yes
Boric acid	No	No	No	No
Borate Buffer	No	-	No	-
Trifluoroacetic acid eluent	No	-	No	-

SEC of chitosan

Aqueous SEC of different chitosan samples dissolved with 3 different solvents was conducted. The pullulan-equivalent number-average and weight-average molar masses M_w and M_n were calculated.

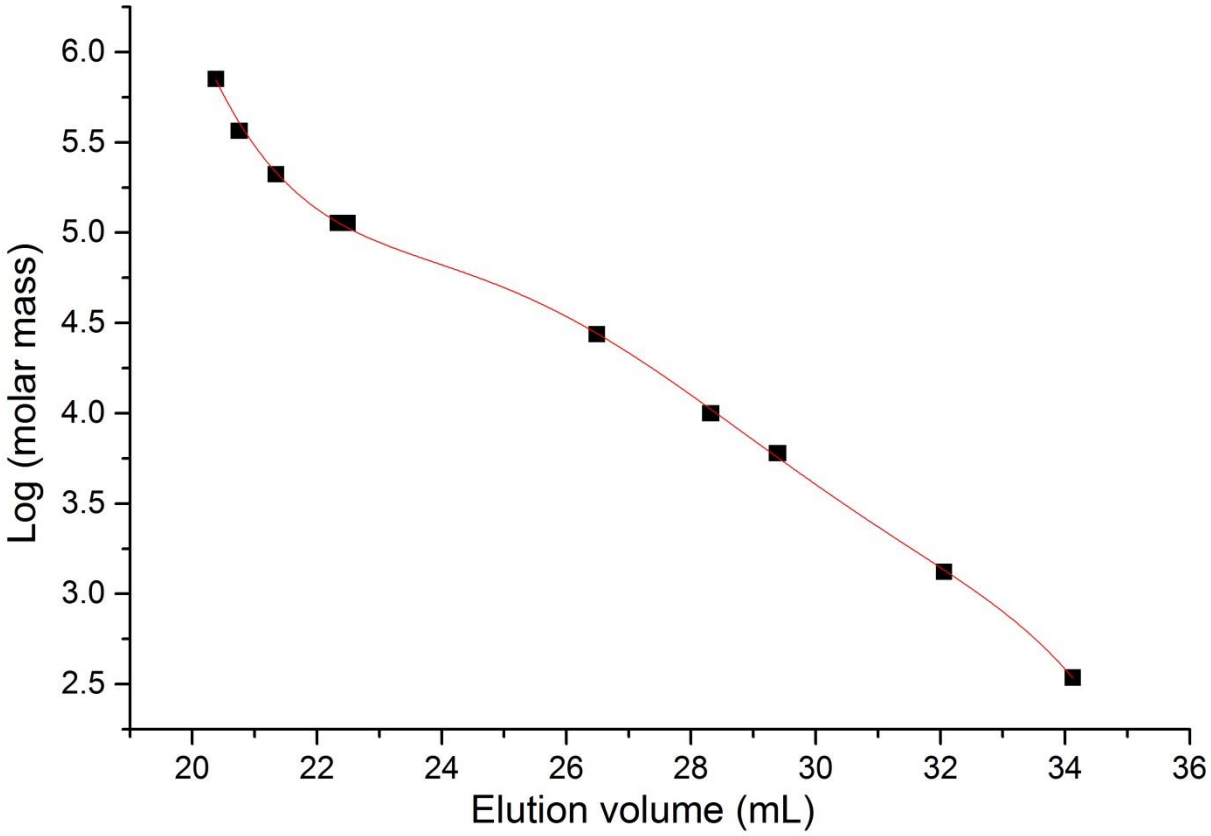

Figure S1: Conventional calibration curve of pullulan standards

Table S3: Pullulan-equivalent M_n and M_w of different chitosan samples injected at different concentrations and dissolved in different aqueous solvents (eluent is composed of 0.3 % (w/v) TFA and 0.1 M NaCl)

Sample	Solvent	Injection concentration ($g \cdot L^{-1}$)	M_n ($g \cdot mol^{-1}$)	M_w ($g \cdot mol^{-1}$)
LowMW1	50 mM HCl	1	830,000	$16{,}000 \times 10^{10}$
		1	1,100,000	$98{,}000 \times 10^{10}$
		1	960,000	$39{,}000 \times 10^{11}$
		1	950,000	$42{,}000 \times 10^{10}$

		0.5	700,000	$77{,}000 \times 10^{12}$
		0.25	950,000	$59{,}000 \times 10^{10}$
	0.3% (w/v) TFA	1	840,000	$55{,}000 \times 10^{10}$
		1	1,100,000	$76{,}000 \times 10^{10}$
		0.5	860,000	$70{,}000 \times 10^{10}$
		0.25	910,000	$17{,}000 \times 10^{10}$
	eluent	1	1,000,000	$91{,}000 \times 10^{10}$
		1	990,000	$76{,}000 \times 10^{10}$
		0.5	1,300,000	$36{,}000 \times 10^{11}$
		0.25	820,000	$17{,}000 \times 10^{11}$
LowMW2	50mM HCl	1	1,400,000	$15{,}000 \times 10^{12}$
		1	1,600,000	$32{,}000 \times 10^{11}$
		0.5	1,600,000	$91{,}000 \times 10^{14}$
		0.25	1,700,000	$90{,}000 \times 10^{10}$
MedMW1	50mM HCl	1	2,100,000	$73{,}000 \times 10^{12}$
		1	3,300,000	$65{,}000 \times 10^{11}$
		0.5	1,600,000	$57{,}000 \times 10^{12}$
		0.25	5,300,000	$62{,}000 \times 10^{13}$
	0.3% (w/v) TFA	1	1,400,000	$41{,}000 \times 10^{12}$
		1	1,600,000	$10{,}000 \times 10^{13}$
		0.5	2,100,000	$90{,}000 \times 10^{11}$
		0.25	4,200,000	$57{,}000 \times 10^{11}$
	eluent	1	1,900,000	$12{,}000 \times 10^{12}$
		1	1,400,000	$85{,}000 \times 10^{12}$
		0.5	1,500,000	$84{,}000 \times 10^{11}$
		0.25	2,300,000	$19{,}000 \times 10^{12}$
MedMW4	50mM HCl	1	1,900,000	$23{,}000 \times 10^{10}$
		1	2,100,000	$51{,}000 \times 10^{12}$
		0.5	1,400,000	$35{,}000 \times 10^{12}$
		0.25	2,000,000	$37{,}000 \times 10^{13}$
MedMW2	50mM HCl	1	1,300,000	$90{,}000 \times 10^{10}$
		0.5	1,900,000	$13{,}000 \times 10^{12}$
		0.25	950,000	$41{,}000 \times 10^{12}$
MedMW3	50mM HCl	1	3,900,000	$38{,}000 \times 10^{14}$
		0.5	1,300,000	$47{,}000 \times 10^{15}$
		0.25	5,400,000	$80{,}000 \times 10^{13}$
Fluk	50mM HCl	1	4,400,000	$65{,}000 \times 10^{13}$
		0.5	5,500,000	$21{,}000 \times 10^{12}$
		0.25	1,300,000	$66{,}000 \times 10^{12}$

Sig	50mM HCl	1	2,900,000	$99{,}000 \times 10^{11}$
		0.5	1,500,000	$48{,}000 \times 10^{12}$
		0.25	3,800,000	$12{,}000 \times 10^{12}$
HighMW	50mM HCl	1	3,600,000	$74{,}000 \times 10^{13}$
		0.5	3,500,000	$31{,}000 \times 10^{12}$
		0.25	1,600,000	$35{,}000 \times 10^{13}$
AKbioD1	50mM HCl	1	930,000	$25{,}000 \times 10^{11}$
		1	920,000	$75{,}000 \times 10^{12}$
		1	940,000	$51{,}000 \times 10^{11}$
		1	910,000	$52{,}000 \times 10^{11}$
		0.5	910,000	$78{,}000 \times 10^{10}$
		0.25	750000	$13{,}000 \times 10^{11}$
AKbioD2	50mM HCl	1	1,500,000	$14{,}000 \times 10^{11}$
		0.5	980,000	$14{,}000 \times 10^{11}$
		0.25	860,000	$50{,}000 \times 10^{11}$
AKbioD3	50mM HCl	1	1,400,000	$70{,}000 \times 10^{10}$
		0.5	1,000,000	$13{,}000 \times 10^{11}$
		0.25	2,300,000	$34{,}000 \times 10^{11}$
AKbioV1	50mM HCl	1	910,000	$54{,}000 \times 10^{10}$
		1	870,000	$40{,}000 \times 10^{10}$
		1	510,000	$97{,}000 \times 10^{10}$
		0.5	730,000	$40{,}000 \times 10^{9}$
		0.25	720,000	$18{,}000 \times 10^{11}$
AKbioV2	50mM HCl	1	2,400,000	$45{,}000 \times 10^{11}$
		0.5	1,900,000	$88{,}000 \times 10^{18}$
		0.25	2,900,000	$11{,}000 \times 10^{13}$
AKbioV3	50mM HCl	1	1,600,000	$12{,}000 \times 10^{13}$
		0.5	2,600,000	$29{,}000 \times 10^{12}$
		0.25	910,000	$57{,}000 \times 10^{12}$

Table S4: Chitosan samples not mentioned in Table 1

Sample	Supplier	Batch number	Catalogue number
HighMW2	Sigma	12913CJ	419419
MedMW3	Sigma	MKBF1336V	448877
MedMW4	Sigma	09303PE	448877
LowMW2	Sigma	06714DJ	448869
Fluk	Sigma (Fluka)	440698/1	28191

Optimization of pressure mobilization of chitosan

Pressure mobilisation was used to assess the dissolution between samples dissolved in 50 mM HCl and AcOH. A number of optimisation steps, mainly of the background electrolyte, were required to analyse the samples.

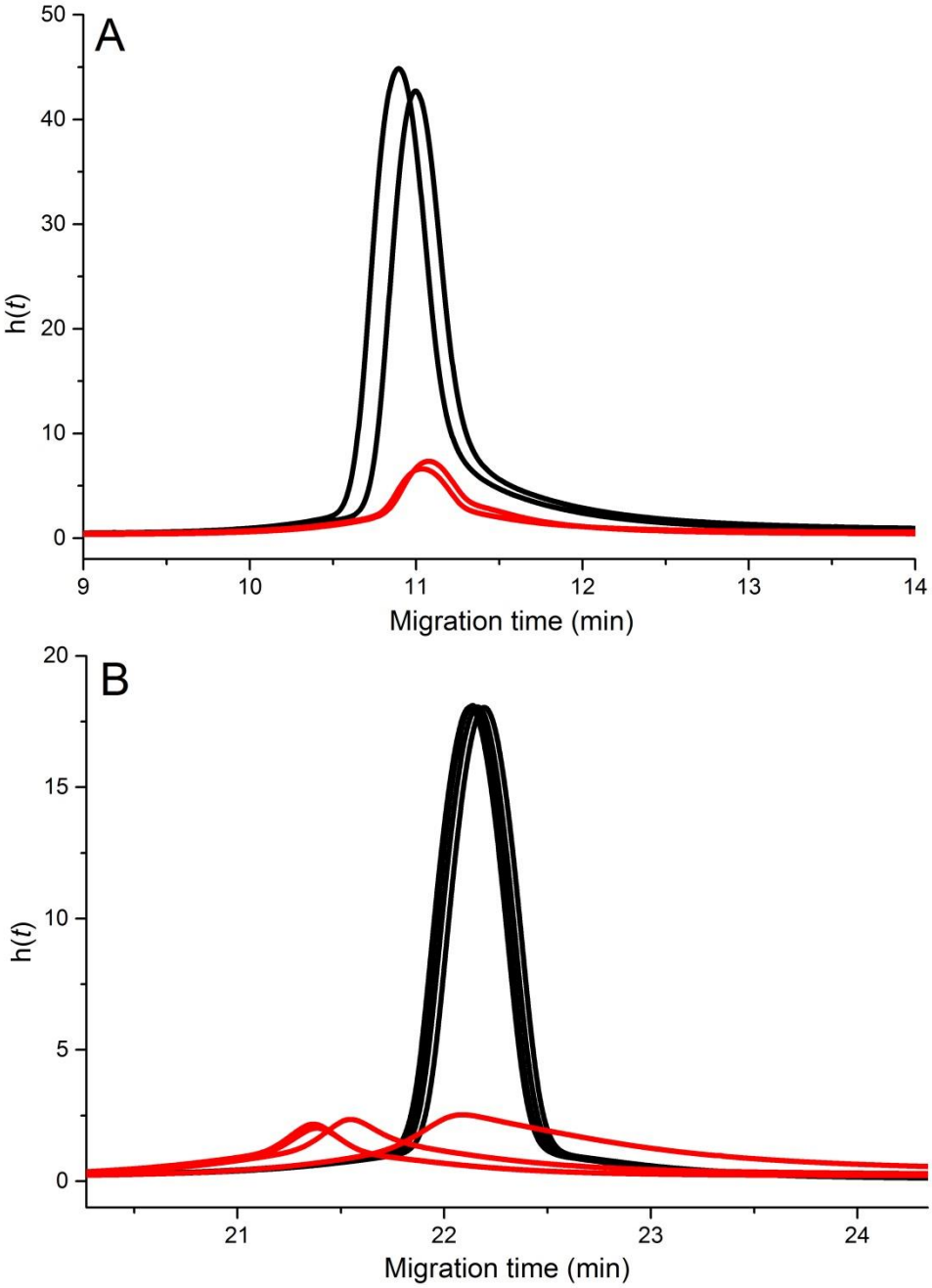

Figure S2: Pressure mobilisation of MedMW1 (no mixing) dissolved in 50 mM HCl (black) and AcOH (red) while the rest of the capillary contains A. phosphate buffer 100 mM pH 3 and at 25 ºC B. phosphate buffer 100 mM pH 2 and at 55 ºC

Mixing using voltage

Pressure mobilization experiments used an inversion of voltage at the start of the experiment to mix the sample with the background electrolyte.

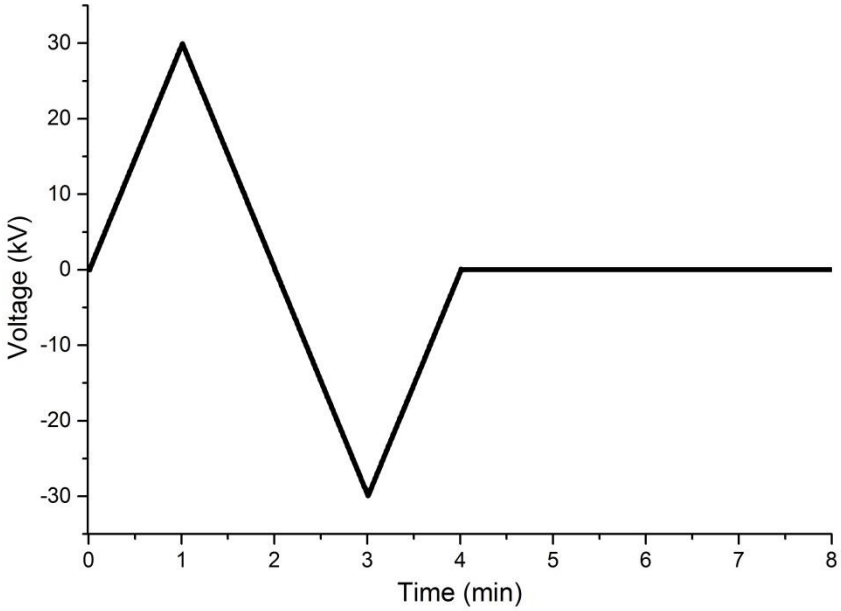

Figure S3: Mixing with inversion of voltage at the beginning of pressure mobilization experiments

Pressure mobilization of chitosan dissolved in aqueous AcOH

A comparison of chitosan dissolved in AcOH using the same conditions as for chitosan dissolved in 50 mM HCl (Fig. 2) produced a narrow peak superimposed on a broader peak. Using the premixing with the electric field as described above did not separate the peak of the chitosan from that of the AcOH solution. Subtracting the peak of AcOH would introduce a large error. It was interesting to note the behavioral differences and interaction of the chitosan with the capillary in different solvents, however, the lack of separation of the narrow peak superimposed onto the chitosan peak prevents an accurate analysis of the dissolution of chitosan in AcOH. (Fig. S4).

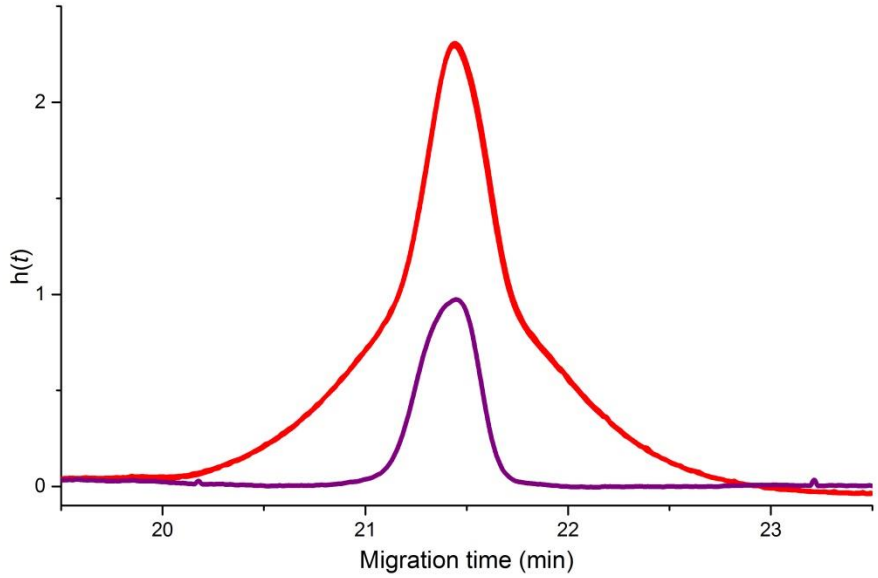

Figure S4: Pressure mobilisation (with mixing) of 50 mM AcOH (purple) and of MedMW1 in 50 mM AcOH (red)

Normalization based on viscosity

To subtract the peak assigned to Cl^-, area normalization was required. The viscosity difference between the chitosan solution and the aqueous HCl (50 mM) was taken into account. The difference between the migration of the apex of the Cl^- peak in the aqueous HCl and the Cl^- peak in the CS solution was measured and used to normalize the y-axis intensity of the Cl^- elugram based on the viscosity difference. The Cl^- peak was then subtracted from the CS elugram.

$$Normalized\ absorbance\ of\ Cl^- = \text{Absorbance of } Cl^- \times \frac{t_2}{t_1} \quad \text{(S1)}$$

Where t_1 is the time at the peak apex of chitosan and t_2 is the time at the peak apex of Cl^-.

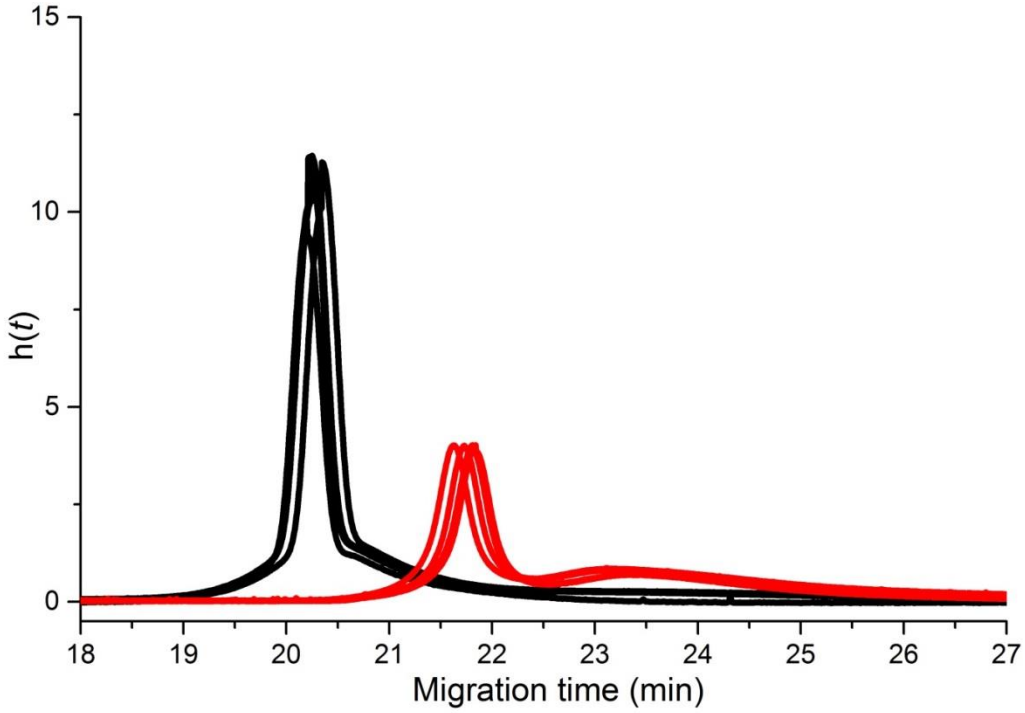

Figure S5: Pressure mobilization of chitosan dissolved in 50 mM HCl (4 black lines) and AcOH (4 red lines) at 55 °C and running in 50 mM HCl and 50 mM AcOH respectively.

Calculation of injection volume for CE and PM experiments

The injection volume *V* is calculated using a rearranged Poiseuille equation as follows:[1, 2]

$$V_t = \frac{\Delta P D^4 \pi}{128 \eta L} \quad \text{(S2)}$$

Where η is the viscosity (1.00 x 10^{-3} kg·m^{-1}·s^{-1}), *L* is the length of the capillary (104 cm total and effective length respectively) , *D* is the diameter of the capillary (50 µm), Δ*P* is the pressure (72 mbar) and *t* is the injection time (10 s).

Correction of raw data

For PM experiments, the y axes of the raw data needs to be time corrected with the following equation:

$$h(t) = \frac{absorbance}{time} \quad \text{(S3)}$$

where absorbance is the raw UV signal obtained from the CE instrument and the time is the x axes obtained from the raw data

For CE experiments both the x and y axes need to be converted to electrophoretic mobility and a weight distribution of electrophoretic mobilities respectively with the following equations:

$$\mu = \frac{l_t l_d}{V}\left(\frac{1}{t_m} - \frac{1}{t_{eof}}\right) \quad \text{(S4)}$$

$$W(\mu) = time \times absorbance \quad \text{(S5)}$$

where l_t and l_d are the length of the capillary and the length to the detector, respectively, *V* is the voltage, t_m is the migration time and t_{eof} is the migration time of a neutral species (electroosmotic flow).

Solution-state NMR spectroscopy

Solution-state NMR spectroscopy measurements were conducted over 61 hours to analyze the behavior of chitosan kept at 60 °C for an extended period of time.

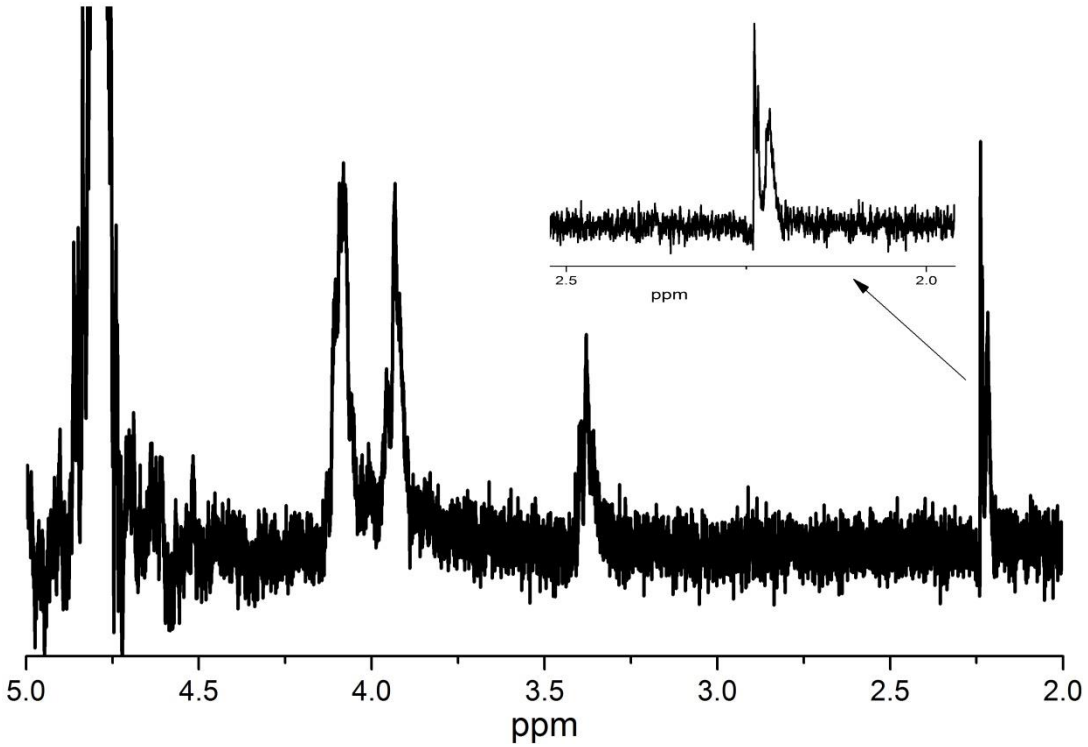

Figure S6. ^{1}H NMR spectrum of chitosan (MedMW1) in D_2O/DCl (50 mM) at 60 °C after several hours

Kinetics of deacetylation

If it obeyed a first order kinetics, the deacetylation of the *N*-acetyl-D-glucosamine unit would follow Eq. S6:

$$\frac{-d[NG]}{dt} = k[NG] \tag{S6}$$

where NG is the *N*-acetyl-D-glucosamine and *t* is the time.

Eq. S6 can be rearranged into

$$\frac{-d[NG]}{[NG]} = k \cdot dt \tag{S7}$$

which integrates into a typical first order kinetics:

$$\ln[NG] - \ln([NG]_\infty) = -kt \tag{S8}$$

Since free AcOH is only created by the deacetylation of NG:

$$[AcOH] = [NG]_\infty - [NG] \tag{S9}$$

Combining Eq. S8 and S9 leads to Eq. S10

$$\ln\left(\frac{[NG]}{[NG]_\infty}\right) = \ln(1 - \frac{[AcOH]}{[NG]_\infty}) = -\mathrm{kt} \tag{S10}$$

Previous solution-state NMR spectroscopy experiments of chitosan

There are several examples of the analysis of chitosan using solution-state NMR spectroscopy. Tabulated below are the various conditions including temperature, solvent and dissolution time.

Table S4: Published examples of conditions for solution-state NMR spectroscopy of chitosan

Year Published, First Author	Solvent	Dissolution Time	Temperature	Reference
1996 Ottoy	1 % v/v AcOH	Overnight	Not specified	[3]
2000 Heux	DCl in D_2O (pH 4)	Not specified	Not specified	[4]
2003 Lavertu	D_2O 1.96 mL + DCl 0.04 mL	30 min	Room temperature	[5]
2014 Dahmane	2 % DCl in D_2O	1 hour	70 ºC	[6]
2014 Lago	1 % CD_3COOD in D_2O	Not specified	not specified	[7]

Signal assignment for ^{1}H NMR spectra of chitosan

To assign the signals of the ^{1}H NMR spectroscopy kinetics, chitosan was dissolved in 50 mM DCl in D_2O for 65 h at 60 °C. The sample was measured and then spiked with 50 mM AcOH and re-measured (Fig. S7). The chemical shift scales were calibrated with the signal of water at 4.717 ppm at 60 °C [8].

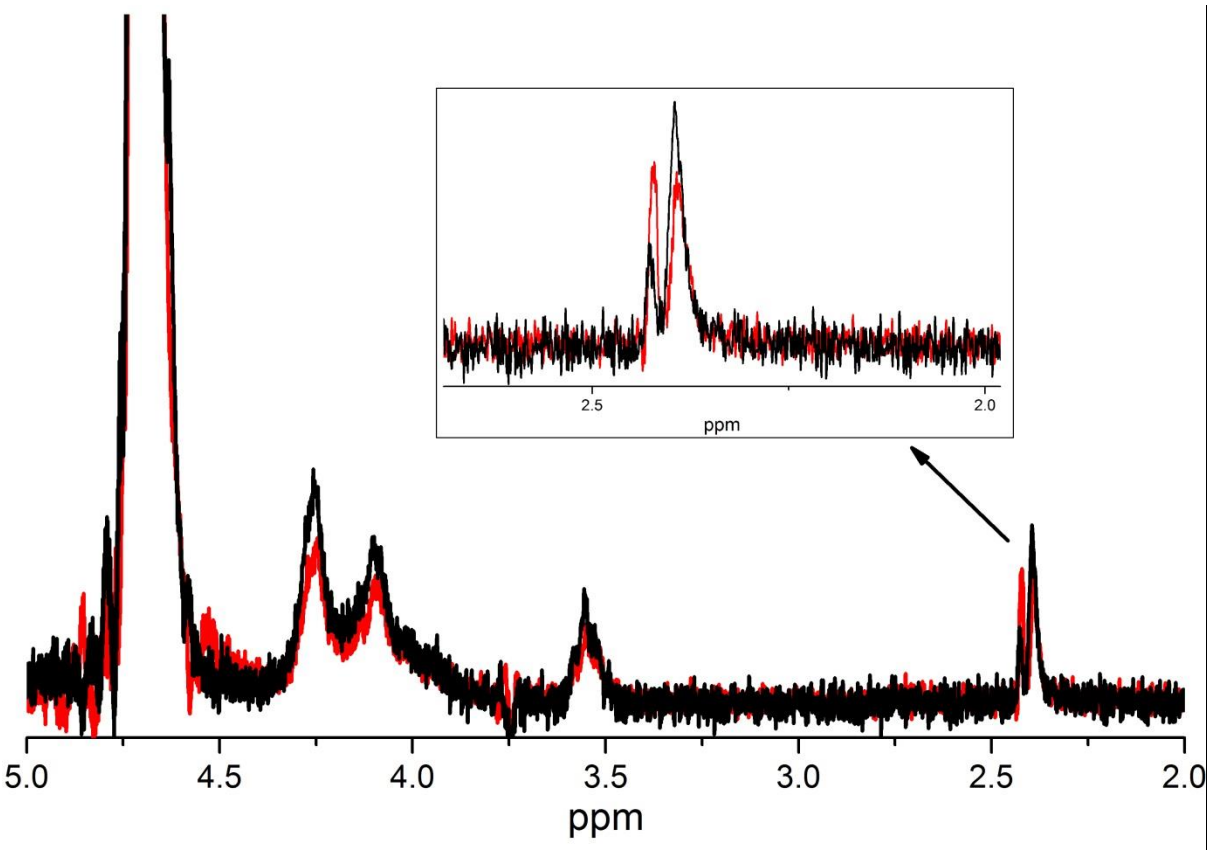

Figure S7. ^{1}H NMR spectrum of chitosan (black line) and chitosan spiked with 50 mM AcOH (red line) dissolved in 50 mM DCl in D_2O.

Magritek Spinsolve benchtop NMR

Solution-state NMR spectra were recorded of chitosan (1 $g \cdot L^{-1}$) prepared in 50 mM DCl in D_2O and 50 mM HCl.

a)

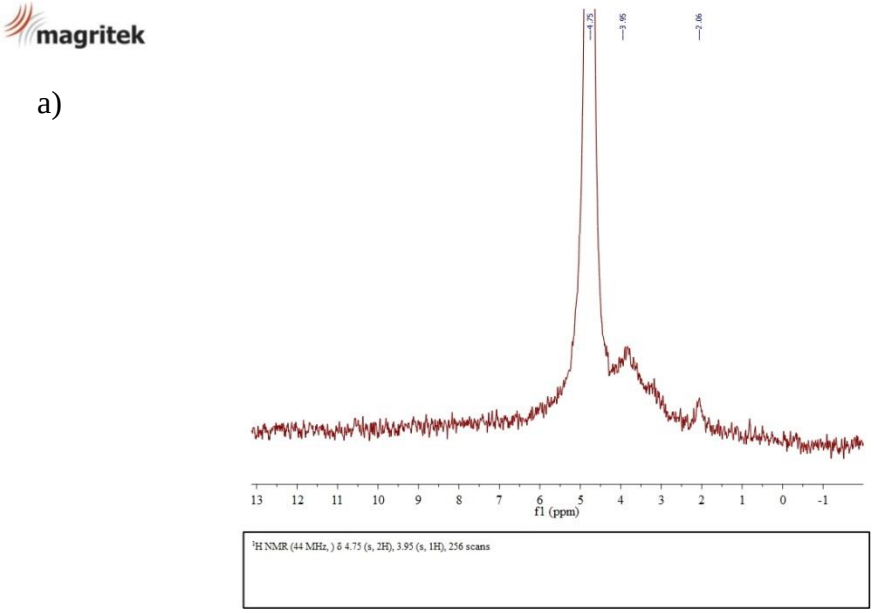

b)

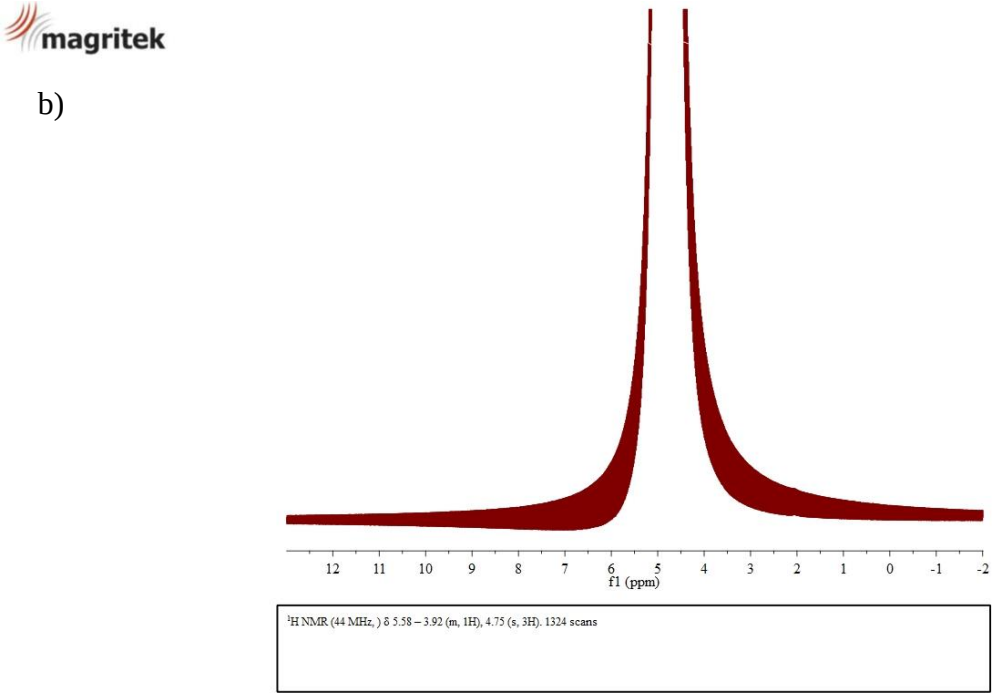

Figure S8. ^{1}H NMR spectrum of chitosan (MedMW1) dissolved in a) 50 mM DCl in D_2O b) 50 mM HCl

Calculation of phasing error on solid-state NMR measurements

The error from phasing was measured by having 4 different users phase 8 different experimental data sets. The results are presented in Table S5.

Table S5. Calculation of error caused by phasing of 8 different solid-state NMR spectroscopy data sets. The *DA* was measured after phasing by 4 different users.

	User - Calculated *DA* (%)						
	1	2	3	4	Average *DA*	*SD*	*RSD* (%)
1	9.53	10.44	8.29	8.30	9.14	1.04	11.41
2	12.09	13.21	11.34	10.56	11.80	1.13	9.56
3	6.85	6.04	6.43	6.44	6.44	0.33	5.14
4	10.27	11.65	10.37	11.07	10.84	0.65	5.97
5	3.48	2.51	2.85	3.43	3.07	0.47	15.23
6	16.34	16.47	16.43	16.51	16.44	0.07	0.45
7	14.24	14.12	14.25	14.87	14.37	0.34	2.35
8	10.73	10.50	10.56	12.36	11.04	0.89	8.05

Kinetics of chitosan dissolution using PACE

The dissolution of chitosan (MedMW1) over time in either 50 mM HCl or 50 mM DCl in D_2O at 60 °C was compared using PACE. The dissolution of different chitosan samples prepared in 50 mM HCl was also compared. The electrophoretic mobility was corrected with both the electroosmotic flow and an additional internal standard. The area was corrected through the integral of the internal standard.

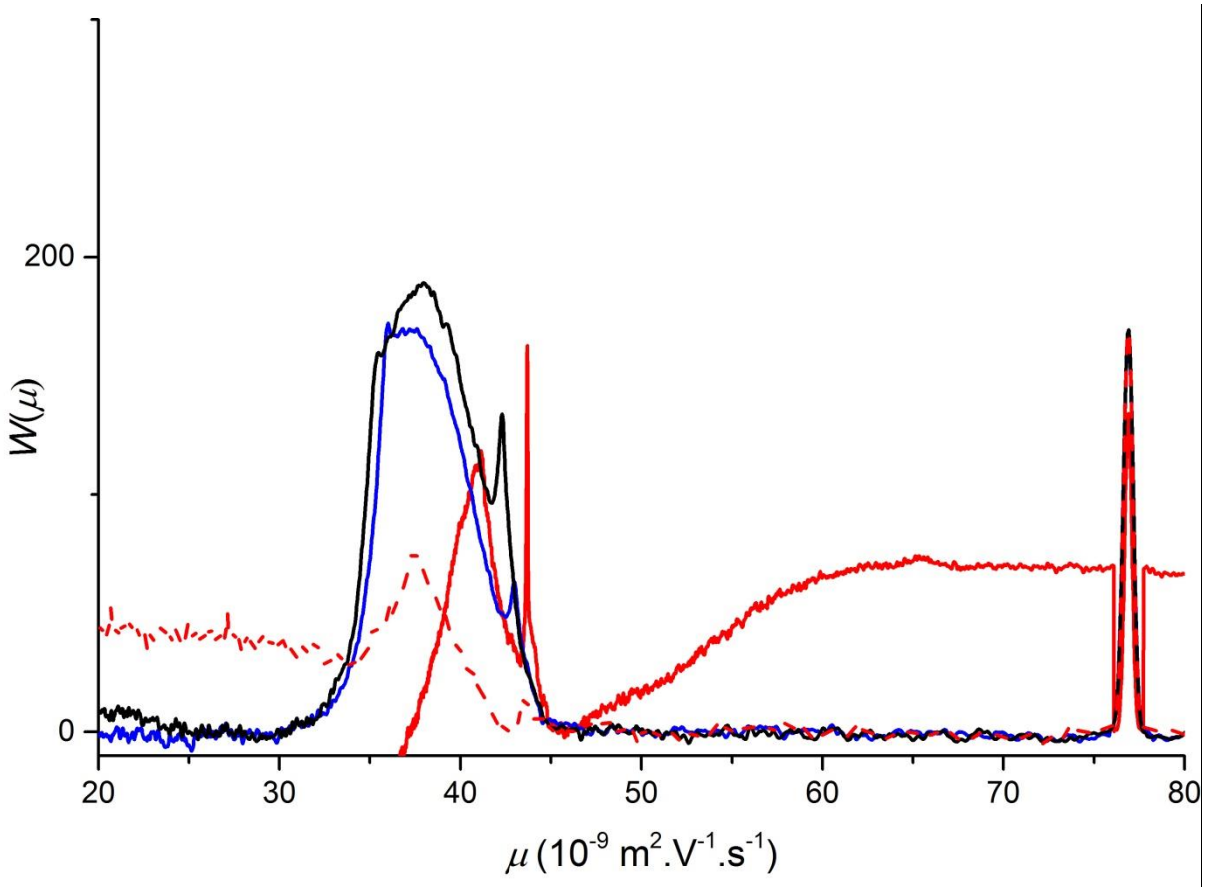

Figure S9. Typical electropherograms of chitosan dissolved in 50 mM DCl in D_2O over 20 hours with a dissolution time of less than 2 h (red lines), 2-10 h (blue line) and 10-20 h (black line).

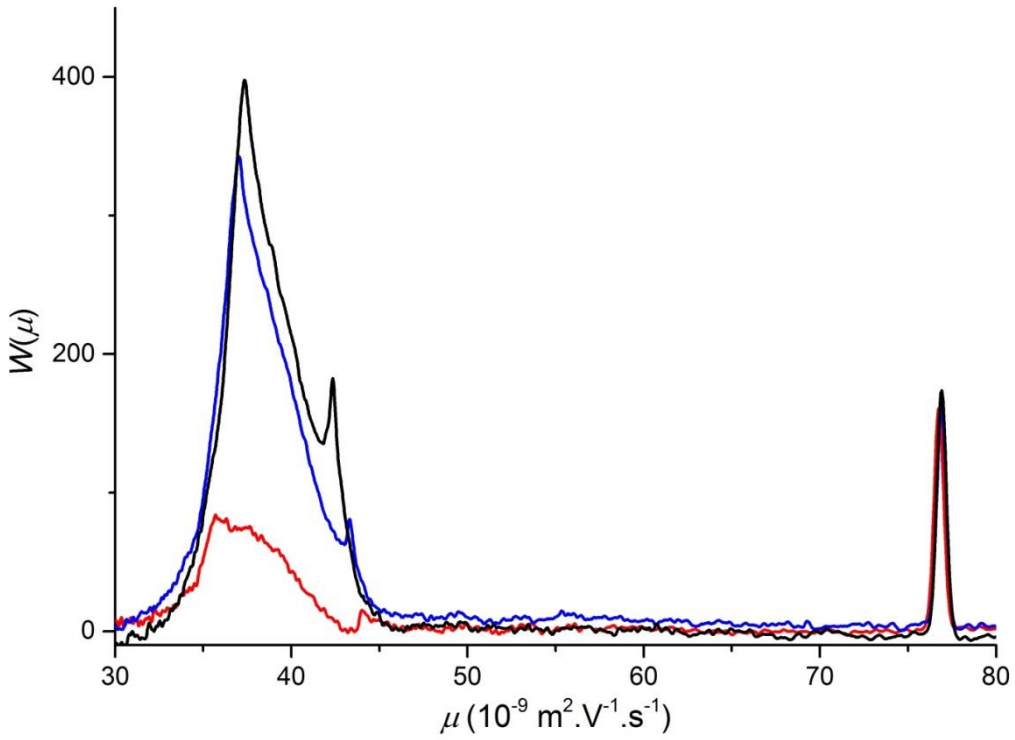

Figure S10. Typical electropherograms of MedMW1 chitosan dissolved in 50 mM HCl over 20 hours with a dissolution time of less than 2 h (red line), 2-10 h (blue line) and 10-20 h (black line).

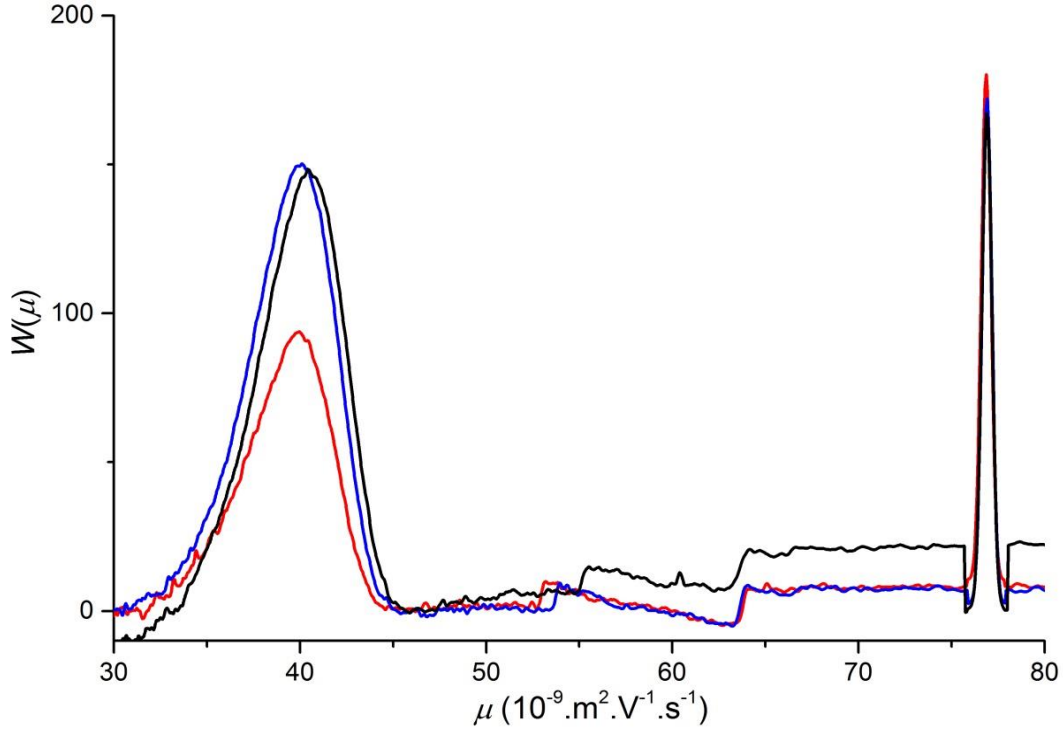

Figure S11. Typical electropherograms of LowMW1 chitosan dissolved in 50 mM HCl over 20 hours with a dissolution time of less than 2 h (red line), 2-10 h (blue line) and 10-20 h (black line).

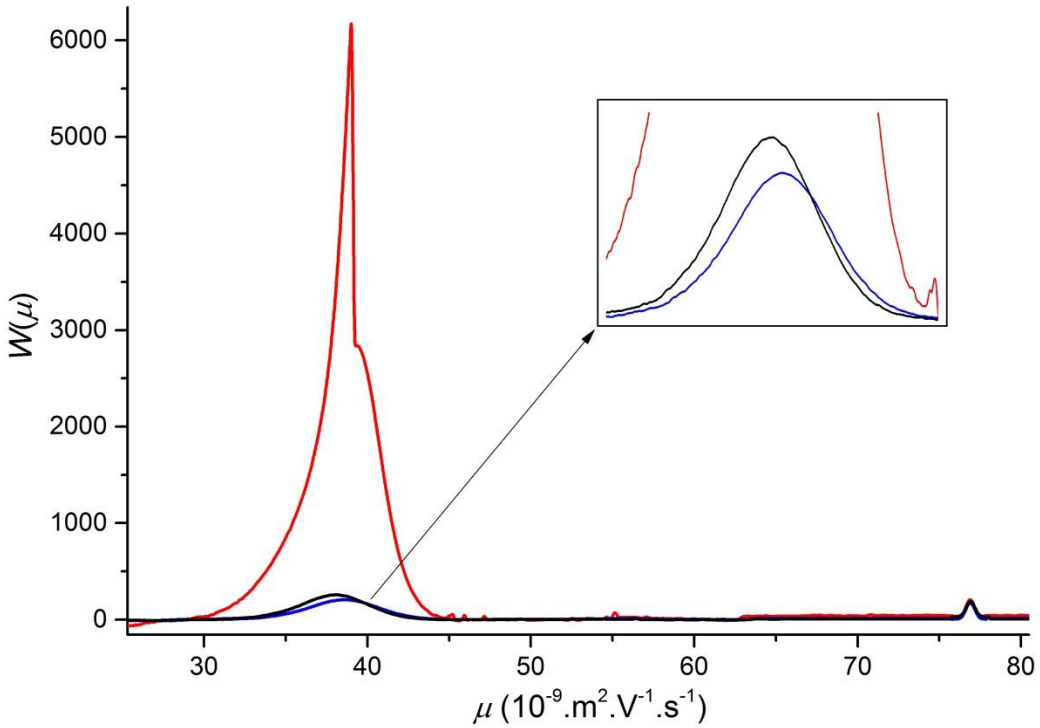

Figure S12. Typical electropherograms of HighMW Par1 chitosan dissolved in 50 mM HCl over 20 hours with a dissolution time of less than 2 h (red line), 2-10 h (blue line) and 10-20 h (black line).

References

[1] G. Taylor, Dispersion of Soluble Matter in Solvent Flowing Slowly through a Tube, Proc. Royal Soc. London A Math. Phys. Sci., 219 (1953) 186-203.

[2] R. Aris, On the Dispersion of a Solute in a Fluid flowing through a Tube, Proceedings of the Royal Society of London Series a-Mathematical and Physical Sciences, 235 (1956) 67-77.

[3] M.H. Ottoy, K.M. Varum, O. Smidsrod, Compositional heterogeneity of heterogeneously deacetylated chitosans, Carbohydr. Polym., 29 (1996) 17-24.

[4] L. Heux, J. Brugnerotto, J. Desbrieres, M.F. Versali, M. Rinaudo, Solid state NMR for determination of degree of acetylation of chitin and chitosan, Biomacromolecules, 1 (2000) 746-751.

[5] M. Lavertu, Z. Xia, A.N. Serreqi, M. Berrada, A. Rodrigues, D. Wang, M.D. Buschmann, A. Gupta, A validated 1H NMR method for the determination of the degree of deacetylation of chitosan, J. Pharma. Biomed. Anal., 32 (2003) 1149-1158.

[6] E.M. Dahmane, M. Taourirte, N. Eladlani, M. Rhazi, Extraction and Characterization of Chitin and Chitosan from Parapenaeus longirostris from Moroccan Local Sources, Int. J. Polym. Anal. Charact., 19 (2014) 342-351.

[7] M.A. Lago, R. Sendon, A.R.B. de Quiros, A. Sanches-Silva, H.S. Costa, D.I. Sanchez-Machado, H.S. Valdez, I. Angulo, G.P. Aurrekoetxea, E. Torrieri, J. Lopez-Cervantes, P. Paseiro, Preparation and Characterization of Antimicrobial Films Based on Chitosan for Active Food Packaging Applications, Food and Bioprocess Technology, 7 (2014) 2932-2941.

[8] R.E. Hoffman, Standardization of chemical shifts of TMS and solvent signals in NMR solvents, Magn. Reson. Chem., 44 (2006) 606-616.